J Physiol 600.23 (2022) pp 5027–5054

The Journal of Physiology

Interdependence of sequential cytotoxic T lymphocyte and natural killer cell cytotoxicity against melanoma cells

Kim S. Friedmann[1], Lea Kaschek[1], Arne Knörck[1], Sabrina Cappello[1,2], Niklas Lünsmann[1], Nadja Küchler[1], Cora Hoxha[1], Gertrud Schäfer[1], Sandra Iden[3], Ivan Bogeski[1,2], Carsten Kummerow[1], Eva C. Schwarz[1] and Markus Hoth[1]

[1]*Biophysics, Center for Integrative Physiology and Molecular Medicine (CIPMM), School of Medicine, Saarland University, Homburg, Germany*
[2]*Molecular Physiology, Institute of Cardiovascular Physiology, University Medical Center, Georg August University, Göttingen, Germany*
[3]*Cell and Developmental Biology, Center of Human and Molecular Biology (ZHMB), School of Medicine, Saarland University, Homburg, Germany*

Handling Editors: Peying Fong & Pawel Ferdek

The peer review history is available in the Supporting Information section of this article (https://doi.org/10.1113/JP283667#support-information-section).

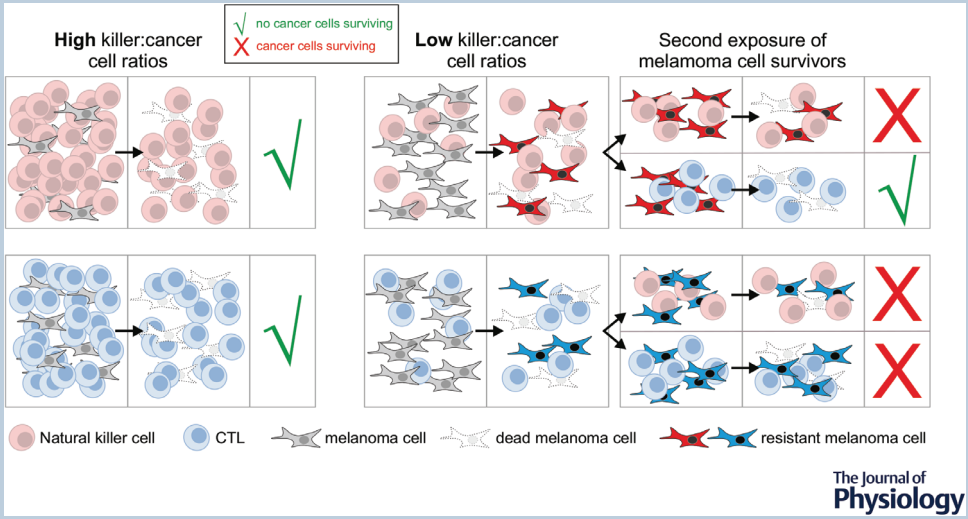

Abstract Cytotoxic T lymphocytes (CTL) and natural killer (NK) cells recognize and eliminate cancer cells. However, immune evasion, downregulation of immune function by the tumour micro-environment and resistance of cancer cells are major problems. Although CTL and NK cells are both important to eliminate cancer, most studies address them individually. We quantified sequential

During her PhD thesis work, **Kim Friedmann** (pictured) established antigen-specific cytotoxic T cell clones. This very time-consuming work was done in close collaboration with the technicians **Cora Hoxha** and **Gertrud Schäfer**. Together with the group leader, **Eva Schwarz**, the four of them designed and optimized the protocols for different and, finally, successful cloning rounds. This work was the basis to test the interdependence of cytotoxic T cell and natural killer cell cytotoxicity against melanoma cells. This exciting but complex project received a lot of guidance, input and help from all the other authors, including the Head of Biophysics, Markus Hoth.

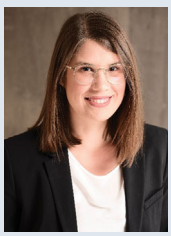

This article was first published as a preprint: Friedmann KS, Knörck A, Cappello S, Hoxha C, Schwär G, Iden S, Bogeski I, Kummerow C, Schwarz EC, Hoth M. 2020. Combined CTL and NK cell cytotoxicity against cancer cells. bioRxiv https://doi.org/10.1101/2020.06.14.150672.

DOI: 10.1113/JP283667

primary human CTL and NK cell cytotoxicity against the melanoma cell line SK-Mel-5. At high effector-to-target ratios, NK cells or melan-A (MART-1)-specific CTL eliminated all SK-Mel-5 cells within 24 h, indicating that SK-Mel-5 cells are not resistant initially. However, at lower effector-to-target ratios, which resemble numbers of the immune contexture in human cancer, a substantial number of SK-Mel-5 cells survived. Pre-exposure to CTL induced resistance in surviving SK-Mel-5 cells to subsequent CTL or NK cell cytotoxicity, and pre-exposure to NK cells induced resistance in surviving SK-Mel-5 cells to NK cells. Higher human leucocyte antigen class I expression or interleukin-6 levels were correlated with resistance to NK cells, whereas reduction in MART-1 antigen expression was correlated with reduced CTL cytotoxicity. The CTL cytotoxicity was rescued beyond control levels by exogenous MART-1 antigen. In contrast to the other three combinations, CTL cytotoxicity against SK-Mel-5 cells was enhanced following NK cell pre-exposure. Our assay allows quantification of sequential CTL and NK cell cytotoxicity and might guide strategies for efficient CTL–NK cell anti-melanoma therapies.

(Received 1 August 2022; accepted after revision 6 October 2022; first published online 13 October 2022)
Corresponding authors Markus Hoth and Eva C. Schwarz: Biophysics, Centre for Integrative Physiology and Molecular Medicine (CIPMM), Building 48, School of Medicine, Saarland University, 66421 Homburg, Germany. Emails: markus.hoth@uks.eu; eva.schwarz@uks.eu

Abstract figure legend Cytotoxic T lymphocytes (CTL) and natural killer (NK) cells eliminate cancer cells. At high killer-to-cancer cell ratios (left row), CTL or NK cells eliminate all melanoma cells, indicating that melanoma cells are initially not resistant to either CTL- or NK cell-mediated cytotoxicity. At low killer-to-cancer cell ratios, CTL or NK cells do not eliminate all melanoma cells (middle row). Sequential second exposure of melanoma cell survivors to fresh CTL or NK cells reveals that pre-exposed melanoma cells are usually not eliminated as efficiently as non-exposed melanoma cells, indicating that pre-exposed melanoma cells acquire resistance to killer cells (right row). Only if secondary CTL exposure follows initial NK cell exposure is cytotoxicity not reduced but, on the contrary, even enhanced.

Key points

- Cytotoxic T lymphocytes (CTL) and natural killer (NK) cells eliminate cancer cells. Both CTL and NK cells attack the same targets, but most studies address them individually.
- In a sequential cytotoxicity model, the interdependence of antigen-specific CTL and NK cell cytotoxicity against melanoma is quantified.
- High numbers of antigen-specific CTL and NK cells eliminate all melanoma cells. However, lower numbers induce resistance if secondary CTL or NK cell exposure follows initial CTL exposure or if secondary NK cell exposure follows initial NK cell exposure. On the contrary, if secondary CTL exposure follows initial NK cell exposure, cytotoxicity is enhanced.
- Alterations in human leucocyte antigen class I expression and interleukin-6 levels are correlated with resistance to NK cells, whereas a reduction in antigen expression is correlated with reduced CTL cytotoxicity; CTL cytotoxicity is rescued beyond control levels by exogenous antigen.
- This assay and the results on interdependencies will help us to understand and optimize immune therapies against cancer.

Introduction

Cytotoxic T lymphocytes (CTL) and natural killer (NK) cells eliminate cancer cells in the human body. There is good evidence for a key role of CTL and NK cells in cancer immune surveillance. Twenty years ago, Imai et al. (2000) found a clear correlation between natural lymphocyte cytotoxicity and cancer incidence in an 11-year follow-up study in the general Japanese population. In addition, Shankaran et al. (2001) reported compelling arguments in favour of this hypothesis when they showed that lymphocytes protect against the development of carcinogen-induced sarcomas. The authors, however, also showed that lymphocytes might select for cancer cells with decreased immunogenicity, which 'explains the apparent paradox of tumour formation in immunologically intact individuals'. Another key finding, by Galon et al. (2006), was that quantification of the type, density and location of immune cells within colorectal cancer samples was a better predictor of patient

survival than commonly used histopathological methods. These and many other reports increased the interest in what is now called the immune contexture or immunoscore of cancer.

The immune contexture of cancer was defined by Fridman et al. (2011, 2017) as the density, composition (including maturation), functional state (functionality) and organization (including location) of the leucocyte infiltrate in a tumour. The immune contexture of cancer is, of course, a key factor shaping the tumour microenvironment, because it influences the concentration of many soluble factors, including cytokines, reactive oxygen species and Ca^{2+} (Frisch et al., 2019). There is also increasing evidence that the immune contexture is correlated with the genomic landscape of cancer as, for instance, recently shown in lung adenomatous premalignancy (Krysan et al., 2019) or breast cancer (Tekpli et al., 2019). In the latter study, the immune contexture defined by the genomic landscape was also correlated with cancer prognosis. According to the summary of data from a large series of publications (summarized by Fridman et al., 2017), $CD8^+$ T cell density in the tumour infiltrate and subtype composition are good prognostic markers for many different cancer types. For NK cells, there is also evidence that cytotoxicity is correlated with cancer incidence. Besides a link between NK cell activity and colorectal cancer (Jobin et al., 2017) or prostate cancer (Kastelan et al., 1997) incidences, Barry et al. (2018) showed that the NK cell frequency is correlated with the abundance of protective dendritic cells in human cancers, including melanoma, and with overall survival. A recent bioinformatics approach on RNA-seq data revealed an improved survival rate for patients with metastatic cutaneous melanoma if tumours showed signs of NK cell infiltration (Cursons et al., 2019). Together, these examples stress the necessity of analysing the interplay of cancer with immune cells, including CTL and NK cells, in detail.

To fight a tumour, CTL or NK cells form a close contact with cancer cells, called an immunological synapse (IS). By direct contact and cytokine release, CTL, NK cells and other immune cells interact with and influence tumours in many ways, often referred to as immunoediting of tumours. This includes the elimination of a tumour as the successful version of immunosurveillance, but it also includes cancer–immune system equilibrium and might also induce the escape of tumours from the immune system in both natural and therapeutic cancer strategies (Muenst et al., 2016).

Immune evasion of cancer is a severe problem that limits CTL and NK cell immune responses in the human body against cancers. Even worse, cancer hijacks certain immune functions for its survival or growth (Hanahan & Weinberg, 2011). To understand immune evasion or resistance of cancer is also of importance to optimize immune responses in the human body through drug-based therapy. In their recent review, Garner and de Visser (2020) state that: '[…] major challenges hinder the progress of immuno-oncology, including a lack of insight into the optimal treatment combinations to prevent or revert resistance to immunomodulatory strategies'. Personalized immunotherapy should integrate CTL and NK cell concepts (Rosenberg & Huang, 2018), stressing the role for study of combined CTL and NK cell cytotoxicity.

Malignant melanoma is a skin cancer with a high mortality rate and increasing incidence worldwide (Schadendorf et al., 2018). High ultraviolet radiation exposure owing to chronic sun-bathing drives mutations in the Trp53 tumour suppressor, thereby accelerating B-Raf proto-oncogene, serine/threonine kinase (BRAF)-dependent melanoma induction (Viros et al., 2014). Recently, ultraviolet radiation mutation signatures have been linked to patient survival (Trucco et al., 2019). Owing to its poor response to many of the standard tumour therapies, including radiotherapy and chemotherapy, treatment options were limited before 2010. The past decade, however, has spawned an enormous evolution in melanoma therapy, bringing both targeted and immunotherapeutic approaches to clinical practice (Jenkins & Fisher, 2020). Patients with mutations in the MAPK pathway might benefit from new molecular targeted strategies, directed against oncogenic BRAF and/or MEK signalling. Moreover, melanoma is a highly immunogenic cancer, which has raised great interest in targeting the immune contexture of this cancer. In physiological conditions, endogenous T cell-driven immune checkpoints control self-tolerance, thereby preventing autoimmunity. Blocking key checkpoint molecules, such as the co-inhibitory receptors cytotoxic T-lymphocyte associated protein 4 (CTLA4), the programmed cell death protein 1 (PD-1) or its ligand PD-L1, can activate CTL to attack cancer. This discovery has led to a breakthrough in development of new cancer treatments (Ribas & Wolchok, 2018). The efficacy of monoclonal antibodies targeting these checkpoint entities has been demonstrated first in melanoma (Brahmer et al., 2012; Hodi et al., 2010).

Meanwhile, immune checkpoint blockade has not only evolved as a first-line treatment strategy for patients with advanced and metastatic melanoma (Jenkins & Fisher, 2020), but is also used as an effective immunotherapy for other cancers (Ribas & Wolchok, 2018). Despite the great advances that immunotherapy has brought to oncological practice, it is important to note that many patients do not respond, whereas others relapse, suggesting yet unknown innate or acquired resistance mechanisms (O'Donnell et al., 2019). Paradoxically, despite eliciting strong immune responses, melanoma cells can frequently evade immune surveillance owing to their high phenotypic plasticity, which is considered one

cause for treatment failure and/or resistance. Melanoma cells undergoing 'phenotypic switching' (e.g. in response to inflammatory mediators) often display considerable non-genomic heterogeneity, suggesting that cancer cell plasticity is, at least in part, a dynamic response to micro-environmental factors (Holzel & Tuting, 2016).

Although the importance of CTL targeting in immunotherapy is, in general, well established, there are also increasing interests and efforts to target NK cells for treatment of melanoma (Cappello et al., 2021; Cursons et al., 2019; Lorenzo-Herrero et al., 2018). In cases where melanoma cells have escaped CTL-mediated elimination, NK cell-based immunotherapy might represent an alternative treatment option (Tarazona et al., 2015). However, the interdependencies of CTL and NK cells in cancer cell cytotoxicity are poorly understood, as are their potential roles in immunotherapy resistance mechanisms.

To gain mechanistic insight into CTL, NK cell and cancer cell interactions, in our study we introduce a simple assay to quantify the sequential efficiency of human CTL and NK cells against melanoma (and, potentially, also against other cancer cell types). We pre-exposed melanoma cells to either CTL or NK cells and analysed the susceptibility of surviving melanoma cells to fresh CTL or NK cells. Conditions that do not allow complete eradication of cancer cells resemble the conditions of an inefficient immune response during cancer development. We found a remarkable resistance of CTL-pre-exposed melanoma cells to subsequent CTL and NK cell-driven cytotoxicity; in contrast, NK cell-pre-exposed melanoma cells were resistant only to further NK cell treatment, whereas subsequent CTL cytotoxicity was even enhanced.

Methods

Ethical approval

This research was approved by the local ethics committee (84/15; Professor Dr Rettig-Stürmer) and conformed to the *Declaration of Helsinki* (apart from registration in a database). The local blood bank within the Institute of Clinical Hemostaseology and Transfusion Medicine at Saarland University Medical Centre provided leucocyte reduction system (LRS) chambers, a byproduct of platelet collection from healthy blood donors. All blood donors provided informed, written consent to use their blood for research purposes.

Cells

T2 cells and lymphoblastoid cell lines were kindly provided by Dr Frank Neumann (José Carreras Centre for Immuno and Gene Therapy, Saarland University, Homburg, Germany) and cultured in RPMI 1640 medium (Thermo Fisher Scientific) supplemented with 10% fetal bovine serum (FBS) and 1% penicillin–streptomycin (Thermo Fisher Scientific). SK-Mel-5 cells were purchased from ATCC (ATCC HTB-70), and a second batch of cells was kindly provided by the Department of Dermatology, Venerology and Allergology (University Hospital of the Saarland, Homburg, Germany), originally purchased from CLS (330 157). SK-Mel-5(B) (originally from CLS) had a passage number that was 30 passages higher than that of SK-Mel-5(A) (from ATCC). The passage number of SK-Mel-5 cells received from ATCC was 30. For comparison in our cell culture, we reduced both passage numbers by 30, meaning that in our cell culture SK-Mel-5 starts at zero. All experiments except the ones in Fig. 5*K–N* and Fig. 3*J, R*, for which CLS was the source as indicated in the figure legend, were performed with SK-Mel-5(A) from ATCC, also called SK-Mel-5 in this paper for simplification. Other melanoma cell lines were from the following sources: 1205Lu (ATCC CRL2806, provided by M. Herlyn, WISTAR Institute, Philadelphia), 451Lu (ATCC CRL2813, provided by M. Herlyn, WISTAR Institute, Philadelphia), SK-Mel-28 (ATCC HTB-72, provided by T. Vogt, Dermatology, Homburg), MeWo (ATCC HTB-65, provided by T. Vogt, Dermatology, Homburg) and MelJuso (DSMZ ACC74, provided by T. Vogt, Dermatology, Homburg). SK-Mel-5 and other melanoma cell lines were maintained in Eagle's minimum essential medium supplemented with 10% FBS and 1% penicillin–streptomycin at 37°C and in humidified air supplemented with 5% CO_2, split twice a week and kept in culture for $\leq$3 months.

Human peripheral blood mononuclear cells (PBMCs) were isolated from healthy donors after routine platelet apheresis using LRS chambers of Trima Accel devices (Institute of Clinical Haematology and Transfusion Medicine, Homburg). For PBMC isolation, density gradient centrifugation using Lymphocyte Separation Medium 1077 (PromoCell) was carried out as described before (Knorck et al., 2018). Primary NK cells were isolated from PBMCs using Dynabead Untouched NK cell isolation kits (Thermo Fisher Scientific) according to the manufacturer's instructions as described previously (Backes et al., 2018). Natural killer cells were cultured at a density of 2×10^6 to 3×10^6 cells/ml in AIM-V (Thermo Fisher Scientific) (+10% FBS) over 5 days for the experiments. On the day of isolation, NK cells were stimulated with 50 U/ml of interleukin (IL)-2. The co-culture assay was usually started on day 1 after isolation and the cytotoxicity assay on day 4 after isolation.

Generation of MART-1-specific $CD8^+$ T cell clones

Melan-A (MART-1, encoded by *MLANA)* specific stimulation of naïve $CD8^+$ T cells of a human

leucocyte antigen (HLA)-A2$^+$ donor was carried out as described previously (Wolfl & Greenberg, 2014). Briefly, immature dendritic cells (DCs) were differentiated from monocytes isolated by plastic adherence. Monocytes were stimulated with IL-4 and granulocyte–macrophage colony-stimulating factor for 72 h, followed by the addition of IL-4, lipopolysaccharide, interferon-γ (IFN-γ) and MART-1 peptide and incubated for 16 h to induce the generation of mature MART-1-presenting DCs. Naïve CD8$^+$ T cells were isolated from autologous PBMCs using a 'Naive CD8$^+$ T Cell Isolation Kit' (Miltenyi Biotec) in parallel to the addition of MART-1 peptide (as described in detail in the Results) to the immature DC fraction. Mature DCs were irradiated with 30 Gy and co-incubated with naïve CD8$^+$ T cells in Cellgro DC medium supplemented with 5% human serum. On the same day, IL-21 was added, whereas IL-7 and IL-15 were applied at day 3, 5 and 7. After 10 days of co-incubation, MART-1-specific stimulation of CD8$^+$ T cells was stopped. CD8$^+$ T cells were re-stimulated with MART-1-loaded autologous PBMCs (irradiated with 30 Gy) for 6 h to induce IFN-γ secretion. Afterwards, antigen-specific CD8$^+$ T cells were isolated using an IFN-γ secretion assay (Miltenyi Biotec). Single cells were seeded into individual wells (1 cell per 200 µl in each well) in RPMI 1640 supplemented with 10% human serum, 1% penicillin–streptomycin, 30 ng/ml anti-CD3 antibody (OKT3, Biolegend), 25 ng/ml IL-2, 5×10^4 heterologous PBMCs per well (mix of two or three donors, irradiated with 30 Gy) and 5×10^4 cells per well of lymphoblastoid cell lines (mix of two donors, irradiated with 120 Gy) in 96-well U-bottomed plates. After 7 days, 50 µl of RPMI 1640 supplemented with 10% human serum, 1% penicillin–streptomycin and 125 ng/ml IL-2 was added to each well. After another week of incubation, proliferating CD8$^+$ T cells were transferred into 25 cm^2 cell culture flasks filled with 20 ml of RPMI 1640 supplemented with 10% FBS, 1% penicillin–streptomycin, 30 ng/ml anti-CD3 antibody (OKT3), 25×10^6 PBMCs (mix of two or three donors, irradiated at 30 Gy) and 5×10^6 cells of lymphoblastoid cell lines (mix of two donors, irradiated at 120 Gy) for expansion of CD8$^+$ T cell clone populations. At day 1, 3, 5, 8 and 11, 30 ng/ml IL-2 and 2 ng/ml IL-15 were added. Finally, antigen specificity was assessed using MART-1-specific dextramers in flow cytometry. Antigen-specific cytotoxicity was analysed using a real-time killing assay (Kummerow et al., 2014). This assay is described in detail below in the subsection 'Short-term (4 h) real-time killing assay'. Antigen-specific clones were frozen in aliquots. Experiments were performed on day 11–14 after thawing and expansion of clonal populations. Cytotoxic T lymphocytes-MART-1 clone 3 (CTL-M3) have been used in another study (Hart et al., 2019).

Reagents

Calcein-AM and CountBright Absolute Counting Beads and $DiOC_{18}$ were purchased from Thermo Fisher Scientific. The following antibodies were used for flow cytometry and stimulation: FITC-labelled anti-HLA-A2 (BB7.2, Biolegend, 1:40), AlexaFluor 647-labelled anti-HLA-A,B,C (W6/32, Biolegend, 1:40), FITC-labelled anti-CD8 (SK1, Biolegend, 1:50), Ultra-LEAF anti-CD3 (OKT3, Biolegend, 30 ng/ml), APC-labelled anti-MART-1 (ELAGIGILTV) dextramers (Immudex, 1:5) and APC-labelled A*0201 dextramer negative control (Immudex, 1:5). Antibodies for western blot: anti-γ-tubulin (Sigma; 1:1000), anti-GAPDH (Cell Signalling; 1:2000) and anti-MART-1 [Agilent/Dako, 1:1000, kindly provided by the Department of Dermatology, Venerology and Allergology (University Hospital of the Saarland, Homburg, Germany)]. 7-Aminoactinomycin D viability staining solution was from Biolegend. MART-1 peptide (MART-$1_{26–35A27L}$) was purchased from JPT. Dulbecco's PBS, 1% penicillin–streptomycin, IL-2, lipopolysaccharide, RPMI 1640, Eagle's minimum essential, AIM-V and CTS-AIM-V media were from Thermo Fisher Scientific. Interleukin-7, IL-15, IFN-γ and IL-4 were from Peprotech. Cellgro DC medium was from CellGenix. Granulocyte–macrophage colony-stimulating factor was purchased from Gentaur. All other reagents were from Sigma-Aldrich.

Pre-exposure of SK-Mel-5 to CTL-M3/NK cells

SK-Mel-5 cells were cultured in minimum essential medium (MEM) supplemented with 10% FBS in 75 cm^2 cell culture flasks (1×10^6 per flask). Immediately before co-culture of SK-Mel-5 and immune cells in AIM-V medium, NK cells and CTL-M3 were irradiated with 30 Gy to prevent proliferation and were added at different effector-to-target (E:T) ratios (indicated in the text) to SK-Mel-5 cells. After 3–4 days, the supernatant was removed, and after a PBS washing step, the remaining SK-Mel-5 cells were harvested for subsequent experiments. We would like to point out that the number of SK-Mel-5 cells increased to a similar extent in AIM-V medium and in MEM, indicating that survival of SK-Mel-5 cells was not impaired in AIM-V compared with MEM.

Western blot

Cell pellets were frozen at −80°C. After thawing, cells were lysed in lysis buffer [150 mM NaCl, 1% Triton X-100, 0.5% NP-40 and 10 mM Tris (pH 7.4)] supplemented with protease inhibitors (complete, EDTA-free; Roche)

and 0.1 µl Benzonase (Sigma-Aldrich). The protein concentration of lysates was quantified using the Pierce BCA (bicinchoninic acid) Protein Assay Kit. Denaturation was carried out in Laemmli buffer at 90°C for 5 min. Seventy-five micrograms of total protein was separated by 15% SDS–PAGE, then transferred onto polyvinylidene difluoride membranes using a transblot transfer chamber (X-Cell SureLock, Invitrogen Novex Mini-cell, or Mini-PROTEAN Tetra Cell, BioRad). Western blots were probed with anti-MART-1 antibodies (1:1000). For the detection of reference genes, blots were probed with anti-γ-tubulin antibodies (1:1000) or anti-GAPDH antibodies (1:2000). Signals were developed in the BioRad imaging system by using ECL solution (Pierce, Thermo Scientific). Densiometric analysis was carried out using the software ImageLab v.5.2.1. and Excel. The expression of protein was normalized to the reference proteins γ-tubulin or GAPDH.

Flow cytometry

Cells (0.5×10^6) were washed in FACS buffer [PBS supplemented with 0.5% bovine serum albumin (BSA)]. Afterwards, cells were stained in 100 µl FACS buffer supplemented with corresponding antibodies and kept in the dark at room temperature for 20 min. After two subsequent washing steps in FACS buffer, the pellet was resuspended in 200 µl FACS buffer and analysed. For dextramer staining, 0.5×10^6 CTL-M3 were washed once in dextramer buffer (PBS supplemented with 5% FBS) and resuspended in 50 µl dextramer buffer. The staining procedure was carried out by adding 10 µl of dextramers with incubation for 10 min in the dark at room temperature. Subsequently, anti-CD8 antibodies were added, and cells were kept in the dark at 4°C for 20 min. After two washing steps, cells were resuspended in 400 µl dextramer buffer and analysed in a BD FACSVerse Flow Cytometer (BD Biosciences). Data analysis was performed using FlowJo (X 10.0.7).

Long-term (>24 h) killing experiments for pre-exposure

For each sample, 5×10^4 SK-Mel-5 cells were seeded in a well of a 48-well plate and incubated in 320 µl MEM supplemented with 10% FBS for 6 h to facilitate adhesion. $DiOC_{18}$ [Live Dead Cell-Mediated Cytotoxicity Kit, L7010 (Thermo Fisher Scientific)] was diluted 1:50 in MEM supplemented with 10% FBS, and 80 µl of $DiOC_{18}$ staining solution was added to each well (the final concentration of $DiOC_{18}$ was 12 µM). After overnight incubation, the staining solution was removed, and cells were rinsed in AIM-V medium supplemented with 10% FBS and incubated in 320 µl AIM-V medium supplemented with 10% FBS for 2 h. Effector cells (5×10^3 to 1×10^6 NK cells or CTL-M3) were added at the indicated E:T ratios of 0.1:1 to 20:1 in a total volume of 80 µl AIM-V medium supplemented with 10% FBS. After 24 h of co-incubation, pictures were taken with a high-content imaging system (ImageXpress, Molecular Devices). Subsequently, cells at the bottom of each well were resuspended and collected in a 5 ml (12 mm × 75 mm) tube. The wells were washed once with PBS supplemented with 0.5% BSA to collect remaining cells. Cells were centrifuged for 5 min at 300*g* and resuspended in 450 µl of PBS supplemented with 0.5% BSA. CountBright Absolute Counting Beads (C36950, Thermo Fisher Scientific; 50 µl) and 5 µl of 7-aminoactinomycin D (Biolegend) were added. After 10 min, analysis was performed on a FACS ARIA III Flow Cytometer (BD Biosciences). We recorded 2×10^3 events of the CountBright Absolute Counting Beads population per sample. Each condition was prepared and recorded in triplicate.

Short-term (4 h) real-time killing assay

To quantify the cytotoxicity of CTL-M3 and primary NK cells, a real-time killing assay was carried out as described before (Kummerow et al., 2014). Briefly, target cells (T2 or SK-Mel-5 cells) were stained with 500 nM Calcein-AM in AIM-V medium supplemented with 10 mM Hepes. In the case of T2 killing or for rescue experiments with SK-Mel-5 cells, the cells were loaded initially in AIM-V medium (supplemented with 10% FBS) with 0.5 µg MART-1 peptide in low-attachment cell culture plates for 1.5 h. After calcein staining, 2.5×10^4 target cells were pipetted per well into 96-well black plates with a clear bottom (VWR/Corning) and kept in the dark for 20 min at room temperature. After settling down of the target cells, effector cells (CTL-M3 or NK cells) were added cautiously at the indicated E:T ratio, and killing was measured in a Genios Pro (Tecan) reader using the bottom reading function at 37°C. Maximal killing rates were calculated as the maximum increase of target lysis between two subsequently measured time points. Maximum target cell lysis was quantified at 240 min.

For each blood donor, we usually compared a control experiment (no pre-exposure) and several experimental conditions side by side to minimize blood donor variability. Owing to NK cell limitations, it was not always possible to compare all experimental conditions for each blood donor. Therefore, we have more data points from blood donors for the control conditions (ctrl) than for the experimental conditions.

Apoptosis–necrosis assay with Casper-GR

The apoptosis–necrosis assay with Casper-GR was essentially carried out as described before (Backes et al., 2018; Knorck et al., 2022). SK-Mel-5 cells were

transiently transfected using the jetOptimus transfection reagent according to the manufacturer's instructions in MEM supplemented with 10% FBS in a 25 cm^2 cell culture flask. The pCasper3-GR vector (Evrogen) was used (2 µg per bottle). After 6 h, the medium was changed to MEM supplemented with 10% FBS plus 1% penicillin–streptomycin and 0.2 µg/ml puromycin. Cells were incubated for 30 h, washed in PBS and BSA, and the pCasper$^+$ (GFP$^+$ RFP$^+$) cells were sorted on a FACS ARIA III sorter (BD Biosciences). The pCasper$^+$ SK-Mel-5 cells were incubated in MEM supplemented with 10% FBS, 1% penicillin–streptomycin and 0.2 µg/ml puromycin overnight. Then 2×10^3 pCasper$^+$ SK-Mel-5 cells per sample were resuspended in 80 µl of CTS AIM-V medium without Phenol Red supplemented with 10% FBS, then seeded in a well of a 384-well black plate. After 2 h resting in the incubator, CTL-M3 or NK cells were added in 20 µl CTS AIM-V medium without Phenol Red supplemented with 10% FBS at the indicated E:T ratios, and cytotoxicity was analysed with the high-content imaging system (ImageXpress, Molecular Devices). Semi-automated analysis was performed using Imaris (Bitplane), ImageJ and Excel.

Cytokine assay

Detection of cytokine profiles in the supernatant was done with the LEGENDplex Human CD8/NK Panel (13-plex) and with the LEGENDplex Human Free Active/Total transforming growth factor-β1 (TGF-β1) assay (BioLegend). Supernatant was collected from the co-culture conditions after 3 days and from the short-term real-time killing assay immediately after the measurement at 4 h. The samples were stored at −80°C. The protocol was carrid out according to manufacturer's instructions, and all conditions were assessed in duplicate. The supernatant collected after the killing assay was diluted 4:1 for the 13-plex assay and 15:1 for the TGF-β1 assay, and the supernatant collected after the co-culture was diluted 3:1 for the TGF-β1 assay, all with the 'assay buffer' provided by BioLegend.

The assay was done with specific antibodies for each cytokine, which were localized on beads that could be differentiated by their size and fluorescence intensity. The kit also provided samples to measure standard curves. The measurement was done with a flow cytometer (BD FACSVerse), and the data were analysed with the LEGENDplex Data Analysis Software Suite by BioLegend.

Statistics

Data are presented as the mean ± SD. If not otherwise stated, n refers to the number of blood donors when experiments were carried out with primary human NK cells, or n refers to the numbers of experiments done with the CTL-M3 clone. All data points represent the average of technical duplicates. Gaussian distribution was tested using the D'Agostino and Pearson normality test. If not stated otherwise, one-way/two-way ANOVA (in the case of Gaussian distribution) or Kruskal–Wallis tests were used to test for significance: $^*P < 0.05$, $^{**}P < 0.01$ and $^{***}P < 0.001$. Statistics were calculated using Prism 7 software (GraphPad Software, La Jolla, CA, USA). The precise P-values are provided in the Statistical Summary document.

Results

Cytotoxic efficiency of MART-1-specific human CTL clones against MART-1-loaded target cells and melanoma cells

The protein MART-1 (melan-A) is often highly expressed in melanoma. The optimal length of the immunodominant peptide was located to the decapeptide MART-$1_{26–35}$ (Romero et al., 1997), which is recognized by HLA-A2-restricted lymphocytes (Kawakami et al., 1994). A change in position 2 from alanine to leucine results in the mutant MART-$1_{26–35A27L}$, which allows a more stable HLA-A2 antigen binding and increased CTL immune responses (Romero et al., 1997). In addition, many T cells from the naïve repertoire express T cell receptors (TCRs) specific for MART-$1_{26–35A27L}$ (Zippelius et al., 2002).

To analyse sequential cytotoxicity of CTL and NK cells against MART-1-positive melanoma target cells, we had to generate MART-1-specific CTL clones from primary human PBMCs. Given that the MART-1 antigen MART-$1_{26–35A27L}$ is specific for the major histocompatibility complex class I serotype HLA-A2, we chose an HLA-A2-positive blood donor to generate MART-1-specific CTL, following a modification of the protocol by Wolfl & Greenberg (2014). We screened and expanded 168 CTL clones from five independent cloning approaches. To test their cytotoxicity, we used T2 and SK-Mel-5 cells as target cells. T2 cells are hybrids of a human T and B cell line and are TAP (transporter associated with antigen processing) deficient but HLA-A2 positive (Salter & Cresswell, 1986). They were chosen because of their TAP deficiency; they cannot transport intrinsic antigens to the cell surface and can thus be loaded easily with different concentrations of exogenous HLA-A2-specific antigens. SK-Mel-5 cells are human melanoma cells and were chosen because they express substantial amounts of MART-1 antigen (Du et al., 2003) and are susceptible to both CTL cytotoxicity (Sugita et al., 1996) and NK cell cytotoxicity (Lee et al., 2011). We confirmed high MART-1 expression of SK-Mel-5 cells by quantification against γ-tubulin expression in

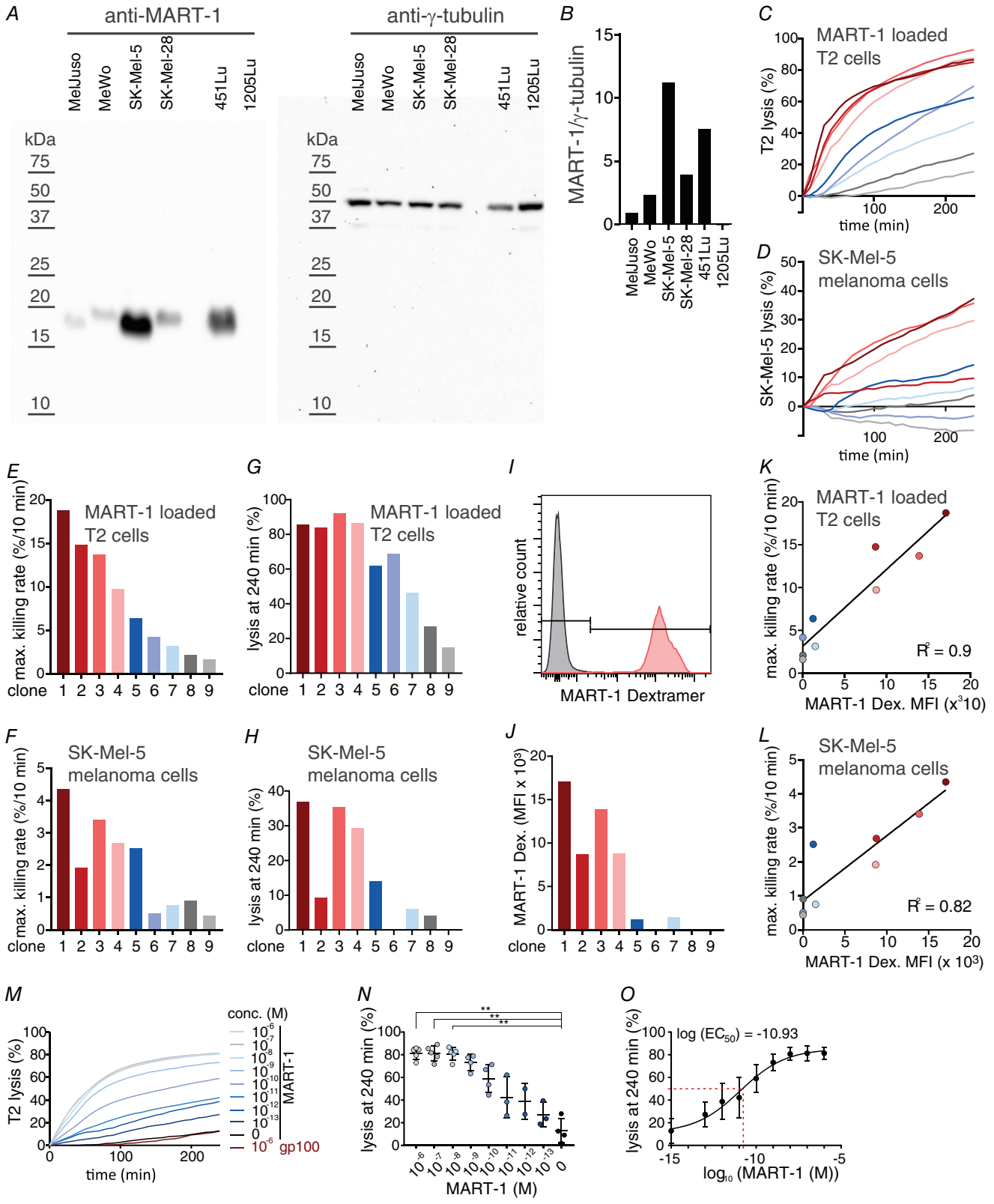

Figure 1. MART-1 expression of different melanoma cell lines and functional analysis of MART-1-specific primary human cytotoxic T lymphocyte clones

A and *B*, western blot analysis of melan-A (MART-1) expression in different melanoma cell lines (*A*) and densitometric quantification against γ-tubulin (*B*). The marker ran in the empty lane between SK-Mel-28 and

451Lu. *C* and *D*, MART-1-specific primary human cytotoxic T lymphocyte (CTL) clones were generated using a modification of the protocol by Wolfl & Greenberg (2014). Different CTL-MART-1 clones show different cytotoxicity against MART-1 peptide-loaded T2 cells (CTL-to-target ratio of 10:1; *C*) or against SK-Mel-5 melanoma cells (CTL-to-target ratio of 20:1; *D*), the latter of which present endogenous MART-1 antigen. *E* and *F*, the maximal killing rate of the CTL-MART-1 clones against MART-1-loaded T2 cells and SK-Mel-5 cells was quantified. *G* and *H*, target cell lysis was quantified after 240 min for MART-1-loaded T2 cells and for SK-Mel-5 cells. *I* and *J*, antigen specificity was quantified using MART-1-specific dextramers in flow cytometry; one example (*I*) and quantification for all clones (*J*) are shown. *K* and *L*, maximal killing rates of CTL-MART-1 clones against MART-1-loaded T2 cells or SK-Mel-5 cells are correlated with the MART-1 dextramer mean fluorescence intensity (Dex. MFI). *M*, to determine functional avidity of cytotoxic T lymphocytes-MART-1 clone 3 (CTL-M3), real-time killing assays were performed with T2 cells loaded with different MART-1 antigen concentrations at an CTL-M3-to-SK-Mel-5 cell ratio of 5:1 ($n = 2$–5). *N*, endpoint lysis at 240 min was quantified and plotted against the corresponding peptide concentration. *O*, data were fitted in a four-parameter Hill equation, revealing a log(EC_{50}) of −10.93 M.

comparison to MelJuso, MeWo, SK-Mel-28, 451Lu and 1205Lu melanoma cells (Fig. 1*A* and *B*).

Figure 1*C*–*L* illustrates the cytotoxicity of nine representative CTL clones and their TCR specificity against MART-$1_{26–35A27L}$ using dextramer technology. These nine clones from one of the five cloning approaches were chosen because their cytotoxicity against MART-1-loaded T2 cells (Fig. 1*C*) covered the full range from ∼90% target elimination over 4 h to <20%. We also tested the cytotoxicity of these nine CTL clones against SK-Mel-5 melanoma cells. In comparison to MART-1-loaded T2 cells, the nine clones were less efficient against SK-Mel-5 cells (Fig. 1*D*), but the relative cytotoxicity of the nine clones against their targets was similar for MART-1-loaded T2 cells and SK-Mel-5 cells. To quantify cytotoxic efficiency against MART-1-loaded T2 cells and SK-Mel-5 cells, we determined maximum killing rates (Fig. 1*E* and *F*) and lysis of targets cells at 240 min (Fig. 1*G* and *H*).

In addition, TCR specificity of the nine clones against MART-$1_{26–35A27L}$ was quantified using dextramer technology. Figure 1*I* shows an example of flow cytometry analysis, which was performed and quantified for all nine clones (Fig. 1*J*). Among the clones, we found a correlation of MART-1-specific TCR expression and cytotoxic efficiency against MART-1-loaded T2 cells (Fig. 1*K*) or SK-Mel-5 cells (Fig. 1*L*). In conclusion, we successfully generated different CTL-MART-1 clones, whose MART-$1_{26–35A27L}$ specificities were correlated with their respective cytotoxic efficiency.

Owing to its high cytotoxicity against MART-1-loaded T2 and SK-Mel-5 cells, CTL_{MART-1} clone 3 was analysed further and tested rigorously for stable cytotoxic efficiency during freezing–thawing cycles. Comparison of the cytotoxic efficiency for different clone expansions after several freezing–thawing cycles revealed a stable overall cytotoxic efficiency against MART-1-loaded T2 cells and even more stable against SK-Mel-5 cells (see also below). Therefore, clone 3 was used throughout the study and is termed CTL MART-1-specific clone 3 (CTL-M3) from now on.

We next characterized the functional avidity of CTL-M3 against T2 cells loaded with different antigen concentrations. Very low cytotoxicity was observed if no antigen was present or if T2 cells were loaded with another common, albeit 'wrong' melanoma-specific antigen, gp100 (Fig. 1*M*, two lowest lines). Cytotoxicity kinetics (Fig. 1*M*) and analysis of the endpoint lysis of target cells (Fig. 1*N*) demonstrated that, within a certain range, elimination of T2 cells by CTL-M3 was highly dependent on the MART-1 antigen concentration. At 10^{-8} M and higher antigen concentrations, cytotoxicity and endpoint lysis did not change any more, indicating saturation beyond 10^{-8} M. A fit of the endpoint lysis with a sigmoidal function revealed a half-maximal antigen concentration of $\sim 10^{-11}$ M (Fig. 1*O*). In summary, we established robust MART-1 antigen-specific CTL that eliminate MART-1-loaded target cells in an antigen dose-dependent manner.

At high E:T ratios, CTL-M3 or NK cells eliminate all SK-Mel-5 cells

A positive prognosis of many cancers is correlated with the number of CTL that have infiltrated the cancerogenic tissue (Fridman et al., 2017), and a similar correlation is predicted for NK cells (Cursons et al., 2019). We tested whether CTL-M3 or primary NK cells are, in principle, able to eradicate all SK-Mel-5 cells completely at a high E:T ratio up to 10:1 or 20:1. We first analysed the survival of SK-Mel-5 cells following 24 h co-culture with different CTL-M3 or NK ratios using a flow cytometry assay. Quantification of these data revealed that few, if any, SK-Mel-5 cells survived the CTL-M3 or NK cell co-culture (Fig. 2*A*). Furthermore, we inspected the cells in parallel by microscopy and did not detect any viable-looking SK-Mel-5 cells after co-culture with CTL-M3 or NK cells (Fig. 2*B*).

To quantify this, we used a single-cell apoptosis–necrosis assay previously established by our group for primary human NK cells (Backes et al., 2018) or CTL (Knorck et al., 2022). SK-Mel-5 cells were transfected with a pCasper-GR construct (a FRET GFP-RFP construct with a caspase3-cleavable site). Viable cells appear orange; they switch to green if apoptosis is induced and lose

fluorescence if necrosis is induced (Fig. 2*C* and *D*). An overview of the whole field of the CTL-M3–SK-Mel-5 cell co-culture is shown in Fig. 2*C*. An example of a successful kill of an SK-Mel-5 cell by a CTL-M3 (indicated by the white arrows; the CTL-M3 is difficult to see because a ×4 objective is used to image the whole well simultaneously) is depicted in Fig. 2*D*. A stacked plot showing the proportion of viable, apoptotic or necrotic cells over time (called a death plot) of all SK-Mel-5 cells from this well reveals that close to 100% of all viable SK-Mel-5 cells are eliminated after 18 h at a 4:1 E:T ratio (Fig. 2*E*). That means that almost all initially viable cells (orange) became either apoptotic (green) or necrotic and lost their fluorescence (grey). We could not recover any viable cells after 3–4 days of co-culture, indicating that a high number of CTL-M3 are able to eradicate all SK-Mel-5 cells.

We repeated the same approach with NK cells at an E:T ratio of 25:1. Again, one complete well was imaged (Fig. 2*F*) and a successful kill is presented, in this case by necrosis, indicated by the loss of fluorescence (Fig. 2*G*). At this high ratio, all SK-Mel-5 cells were killed by either necrosis or apoptosis after 2 h (Fig. 2*H*). We noticed that both CTL-M3 and NK cells sometimes killed by apoptosis followed by secondary necrosis, as indicated by the smaller number of apoptotic (green) SK-Mel-5 cells towards the

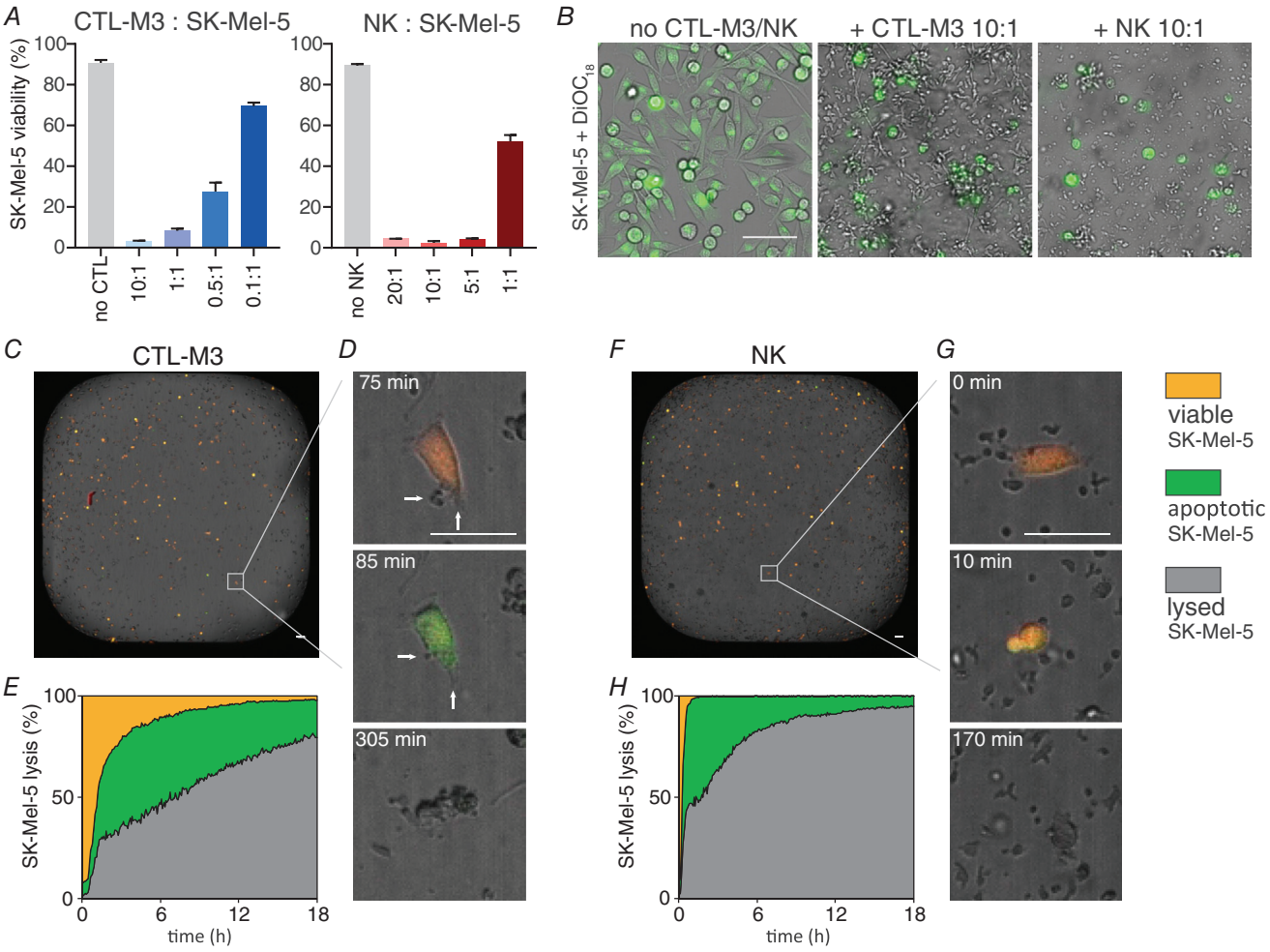

Figure 2. Cytotoxic T lymphocytes-MART-1 clone 3 or natural killer cells both completely eradicate SK-Mel-5 cells at high effector-to-target ratios
A, flow cytometry analysis of cytotoxic T lymphocytes-MART-1 clone 3 (CTL-M3) or natural killer (NK) cell cytotoxicity at different effector-to-target (E:T) ratios, respectively, against SK-Mel-5 cells. *B*, images of 5×10^4 $DiOC_{18}$-labelled SK-Mel-5 cells co-cultured with CTL-M3 (E:T ratio of 10:1) or NK cells (E:T ratio of 10:1) for 24 h in a 48-well plate. *C–H*, real-time killing assays with 2×10^3 transiently Casper-GR-transfected SK-Mel-5 cells in a 384-well plate. The whole field of view, with all cells, was analysed with the high-content imaging system. Overview of the complete well of SK-Mel-5 cells transiently transfected with Casper-GR incubated with CTL-M3 cell at an E:T ratio of 4:1 (*C–E*) or with NK cells at an E:T ratio of 25:1 (*F–H*). *D* and *G*, example of successful killing of a SK-Mel-5 cell by a CTL-M3 (*D*, white arrows) or an NK cell (*G*). *E* and *H*, death plot of SK-Mel-5 cells of the whole well in the presence of CTL-M3 (*E*) or NK cells (*H*). Scale bars: 100 µm.

end of the experiment compared with an earlier time point between 1 and 2 h (Fig. 2*E* and *H*).

We conclude that CTL-M3 or NK cells both eradicate all SK-Mel-5 cells in the culture at high E:T ratios. This finding implies that there are no resistant SK-Mel-5 cells present in the initial co-culture.

A co-culture assay to analyse combined CTL-MART-1 and NK cell cytotoxicity against melanoma

To fight cancer, it would be beneficial to maintain high killer cell-to-cancer cell ratios in cancer tissue, because these are correlated with the outcome. Unfortunately, it seems unlikely that E:T ratios of CTL- or NK-to-cancer cells of 10:1 or higher are present in cancer tissue in the human body. Instead, lower E:T ratios have been reported for NK cells in many cancers, including melanoma lesions (Balsamo et al., 2012).

In contrast to many assays published so far, CTL and NK cells do not fight cancer independently of each other in the human body. To analyse sequential CTL-M3 and NK cell cytotoxicity against the same cancer, in this case melanoma SK-Mel-5 cells, we designed a suitable experimental set-up (Fig. 3*A* and *B*). We established a co-culture assay, in which irradiated NK cells or CTL-M3 were used for pre-incubation to avoid their further proliferation during co-culture. Irradiated CTL-M3 or NK cells kill as efficiently as their non-irradiated counterparts (Fig. 3*C* and *D*). SK-Mel-5 cells were pre-exposed to irradiated CTL-M3 or NK cells during co-culture at different E:T ratios for 3–4 days (Fig. 3*A*). Following this CTL-M3 or NK cell pre-exposure during co-culture, we quantified the cytotoxicity of fresh, non-irradiated CTL-M3 or NK cells against surviving SK-Mel-5 cells, resulting in four different possible experimental combinations (Fig. 3*B*): (i) NK cell cytotoxicity after NK cell pre-exposure during co-culture; (ii) CTL-M3 cytotoxicity after NK cell pre-exposure during co-culture; (iii) NK cell cytotoxicity after CTL-M3 pre-exposure during co-culture; and (iv) CTL-M3 cytotoxicity after CTL-M3 pre-exposure during co-culture. The cytotoxicity of fresh CTL-M3 or NK cells was finally quantified using a kinetic 'real-time' killing assay (Kummerow et al., 2014).

We characterized several important parameters of this assay. First, we analysed proliferation of SK-Mel-5 cells in various conditions. In control conditions, SK-Mel-5 cells proliferated with a factor of ∼1.5/day from 1×10^6 cells initially to 3.4×10^6 cells after 3 days with no killer cells present (Fig. 3*E*). With NK cells present at a ratio of 2:1, the number of SK-Mel-5 cells decreased to 2.3×10^6 after 3 days. This means that <20% of living SK-Mel-5 cells were killed each day in the culture. With CTL-M3 present at a ratio of 1:1, proliferation and killing of target cells was balanced, with 0.97×10^6 SK-Mel-5 cells in the co-culture after 3 days.

Second, we wanted to test the reproducibility (or robustness) of the assay. The main parameters that are varied during the assay are the three cell types: primary NK cells, CTL-M3 clones and SK-Mel-5 target cells. To overcome variability of primary NK cells, we decided always to analyse several blood donors. Regarding the other two cell types used, we tested the reproducibility (robustness) experimentally. To test robustness of CTL-M3 cytotoxic efficiency against SK-Mel-5 target cells, we compared different expansions that we needed to obtain sufficient numbers of CTL-M3 for this study and future studies. Comparison of the cytotoxic efficiency of CTL-M3 for different expansions revealed that the cytotoxic efficiency was stable, with no significant differences regarding overall lysis (Fig. 3*F*), maximal lysis after 240 min (Fig. 3*G*) or maximal killing rate (Fig. 3*H*).

To test the robustness of SK-Mel-5 cells as a target cell type over time is another important aspect. An especially important parameter is the expression of the antigen MART-1, which is highly variable in melanoma. We tested MART-1 expression during extended times of SK-Mel-5 cell culture. For these experiments, we used two diverse sources of SK-Mel-5 cells with different passage numbers: SK-Mel-5(A) from ATCC and SK-Mel-5(B) from CLS. We used those because they already had different passage times [SK-Mel-5(B) was 30 passages higher] and differential MART-1 expression, which declined further over additional passage numbers (Fig. 3*I* and *J*). Quantification against γ-tubulin revealed a good inverse correlation of MART-1 expression with passage numbers (Fig. 3*K*). We next quantified the cytotoxic efficiency of CTL-M3 against SK-Mel-5 with different passage numbers. As expected, cytotoxicity declined with increasing passage numbers and decreasing MART-1 expression (Fig. 3*L*–*N*). We also tested the efficiency of primary NK cells against SK-Mel-5 cells with different passage numbers. Also in this case, cytotoxic efficiency dropped at passage numbers >30 (Fig. 3*O*–*Q*). Given the robustness of CTL-M3 and NK cell cytotoxicity against SK-Mel-5 cells up to passage number 30, we decided to use SK-Mel-5 cells only up to passage number 30 in the whole study, apart from one data set designed to check the effect of low MART-1 expression (Fig. 5*K*–*N*, see below). Figure 3*R* summarizes the data of Fig. 3*I*–*Q* by correlating the MART-1 expression and cytotoxicity for both NK cells and CTL-M3. It is evident that CTL-M3 cytotoxicity is correlated with MART-1 expression, whereas there is only a low correlation with NK cell cytotoxicity. The latter might be caused by additional changes to surface receptors in SK-Mel-5 cells at high passage numbers that we did not explore in any further detail. In summary, we verified that the assay reveals reproducible results for both primary NK cells and CTL-M3 clones when SK-Mel-5

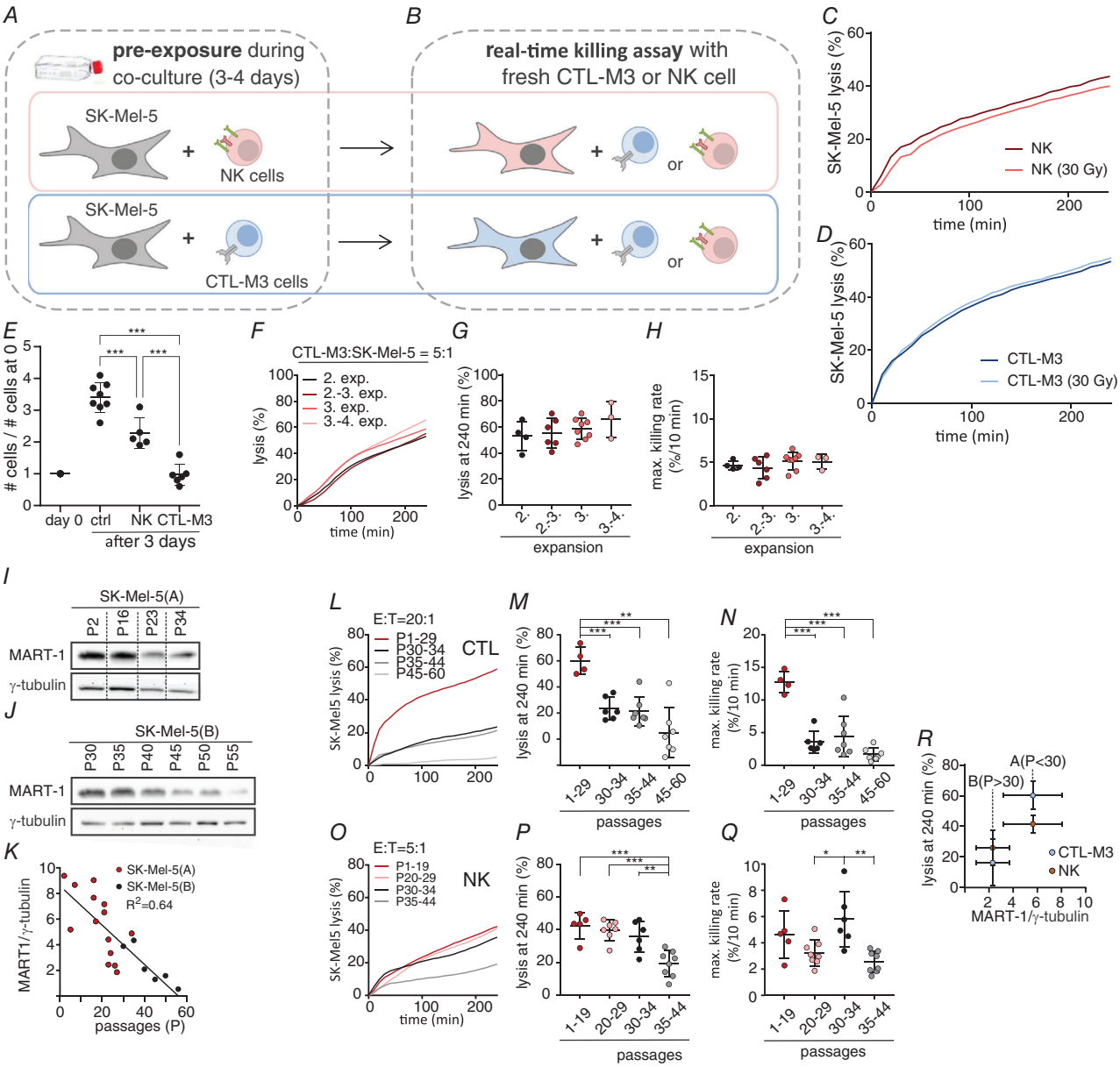

Figure 3. A co-culture assay to analyse the interdependence of cytotoxic T lymphocytes-MART-1 clone 3 and natural killer cell cytotoxicity against SK-Mel-5 melanoma cells
A, 10^6 SK-Mel-5 cells were co-cultured for 3–4 days together with irradiated cytotoxic T lymphocytes-MART-1 clone 3 (CTL-M3) or primary natural killer (NK) cells at different effector-to-target (E:T) ratios, respectively. *B*, SK-Mel-5 cells that survived CTL-M3 or NK cell pre-exposure were harvested, then subjected to fresh CTL-M3 or NK cells and analysed by the real-time killing assay. Colour-coded scheme: orange-labelled cells depict SK-Mel-5 cells previously pre-exposed to NK cells; blue-labelled SK-Mel-5 cells depict SK-Mel-5 cells previously pre-exposed to CTL-M3. *C* and *D*, irradiated (30 Gy) CTL-M3 or NK cells eliminate SK-Mel-5 cells as efficiently as non-irradiated CTL-M3 or NK cells at an E:T ratio of 10:1. *E*, number of SK-Mel-5 cells after 3 days relative to the number of cells seeded into each flask at day 0 (10^6 SK-Mel-5) with no killer cells present (ctrl), with NK cell present at a ratio of 2:1 or with CTL-M3 present at a ratio of 1:1 (n = 5–7). *F–H*, analysis of the cytotoxic potential of CTL-M3 between different expansions; averaged lysis kinetics of SK-Mel-5 cells (*F*), lysis at final time point at 4 h (*G*) or maximal killing rate (*H*) as measured with the real-time killing assay (n = 3–8). *I* and *J*, MART-1 protein expression analysis of SK-Mel-5 cells cultured for different passage times (n = 1–7 repetitions). Bands that were not at first directly adjacent are shown separated by dotted lines (in *I*). *K*, correlation of normalized MART-1 protein expression with passage number of SK-Mel-5 cells. *L–Q*, plots of averaged lysis kinetics (*L*), lysis at the final time point of 4 h (*M*) and maximum killing rate of SK-Mel-5 cells (*N*) with different passages by CTL-M3 (n = 4–7) or primary NK cells (*O–Q*, n = 5–8) measured with the real-time killing assay. *R*, correlation of averaged lysis at end time point at 4 h by CTL-M3 or NK cells, respectively, with MART-1 expression in SK-Mel-5 cells with passage times <30 or >30 (A and B refer to the cells shown in *I* and *J*).

cells are used at low passage numbers below passage number 30.

Although *in vitro* assays for human cells can obviously not mimic the tumour microenvironment, we nevertheless characterized the *in vitro* environment of the assay regarding different cytokines (Fig. 4*A*–*C*) and cytotoxic effector molecules (Fig. 4*D*–*F*) released into the medium. Considering cytokines, we analysed: (i) IL-2, which is mainly secreted by $CD4^+$ T cells but also by other immune cells, including CTL and NK cells, and which has many important effector functions, including the enhancement of CTL and NK cell proliferation and activity (Hernandez et al., 2022); (ii) IFN-γ, which is released by many different immune cells, including CTL and NK cells, and has mostly (but not exclusively) anti-tumorigenic effects (Gocher et al., 2022); (iii) tumor necrosis factor-α (TNF-α), which is mainly produced by macrophages and T cells but also by other immune cells and which is considered a strong pro-inflammatory mediator also involved in tumorigenesis (Ochayon & Waggoner, 2021); (iv) immunoregulatory cytokines, such as IL-10 and TGF-β, which are also produced by CTL and NK cells (Ochayon & Waggoner, 2021). In addition, we analysed four of the most important cytotoxic effector proteins released by CTL and NK cells into the medium: perforin, granzyme A, granzyme B and granulysin (Prager & Watzl, 2019).

We focused our analysis on the two most relevant conditions, analysing the concentrations of cytokines and cytotoxic molecules in the medium at the end of NK cell-induced killing after CTL-M3 pre-exposure or at the end of CTL-M3-induced killing after NK cell pre-exposure. In some cases, we also analysed cytokine concentrations at the end of the pre-incubation.

Regarding IL-2, no significant differences were seen at the end of NK killing regardless of whether SK-Mel-5 cells were pre-exposed to CTL-M3 or not (Fig. 4*A*). There was a slight drop when NK cells were used at 5:1, which was, however, not seen at 10:1. During CTL-M3 killing of SK-Mel-5 cells pre-exposed to NK cells, higher IL-2 concentrations were measured in general, but also in this case there were no significant differences, regardless of whether or not SK-Mel-5 cells were co-cultured with different numbers of NK cells (Fig. 4*B*). At the end of the co-culture with NK cells, IL-2 concentrations were not increased compared with SK-Mel-5 target cells only, regardless of whether NK cells were incubated with IL-2 or not or whether they were irradiated or not (Fig. 4*C*). At the end of the co-culture with CTL-M3, IL-2 concentrations were slightly elevated (Fig. 4*C*), in line with the experiments shown in Fig. 4*B*. For IFN-γ and TNF-α, the results were similar, with more IFN-γ and TNF-α produced by CTL-M3 than by NK cells; however, again, pre-incubation did not change the cytokine concentrations for any of the conditions (Fig. 4*A*–*C*). Interleukin-10 and TGF-β concentrations were not increased (Fig. 4*A*–*C*). For TGF-β, the values were identical for different conditions because they were not above the detection limit in any of the conditions. For IL-10, values were not over or barely over the detection limit.

Regarding the cytotoxic effector proteins perforin, granzyme A, granzyme B and granulysin, we did not observe any significant differences during NK cell or CTL-M3 killing for any of the pre-exposure conditions in comparison to control conditions (Fig. 4*D* and *E*). As expected, their concentrations were higher at the end of pre-exposure with CTL-M3 or NK cells in comparison to control conditions with only SK-Mel-5 cells present. In this case, non-irradiated CTL-M3 produced about twice the amount of cytotoxic effector molecules as irradiated CTL-M3 (Fig. 4*F*).

Natural killer cell and CTL-M3 cytotoxic efficiency against melanoma cells surviving NK cell pre-exposure

Applying the assay described in Fig. 3, we incubated NK cells and melanoma cells at E:T ratios that did not eliminate all melanoma cells within 3–4 days. Subsequently, the cytotoxicity of fresh CTL-M3 or NK cells against surviving SK-Mel-5 was quantified (Figs 5 and 6).

It was shown that melanoma cells acquired a protected phenotype against fresh human NK cells after surviving a long-term co-culture with low numbers of NK cells (Balsamo et al., 2012; Huergo-Zapico et al., 2018). Testing the NK cell cytotoxicity of fresh NK cells against melanoma cells surviving pre-exposure to insufficient numbers of NK cells was done as a proof-of-principle experiment. During the 3- to 4-day-long primary encounter, NK cell-to-SK-Mel-5 cell (NK:SK-Mel-5) ratios were varied between 2:1 and 8:1, including a control with no NK cells but with NK cell medium (Fig. 5*A*). Following this primary encounter, the surviving SK-Mel-5 cells were exposed to fresh NK cells at an NK:SK-Mel-5 ratio of 5:1, and cytotoxicity was analysed (Fig. 5*B*). Quantification of the maximal killing rate and the lysis at the end of the experiment revealed that the efficiency of fresh NK cells to eliminate surviving SK-Mel-5 cells was reduced at higher NK:SK-Mel-5 ratios during pre-exposure (Fig. 5*C* and *D*). Comparable results were obtained in independent experiments with different blood donors if surviving SK-Mel-5 cells were exposed to fresh NK cells at a ratio of 10:1 (Fig. 5*G*–*J*). For these blood donors, NK cell cytotoxicity was not as high as for the ones used in Fig. 5*B* and *C*; however, the results were the same, in that the efficiency of fresh NK cells to eliminate surviving SK-Mel-5 cells was reduced at higher NK:SK-Mel-5 ratios during pre-exposure.

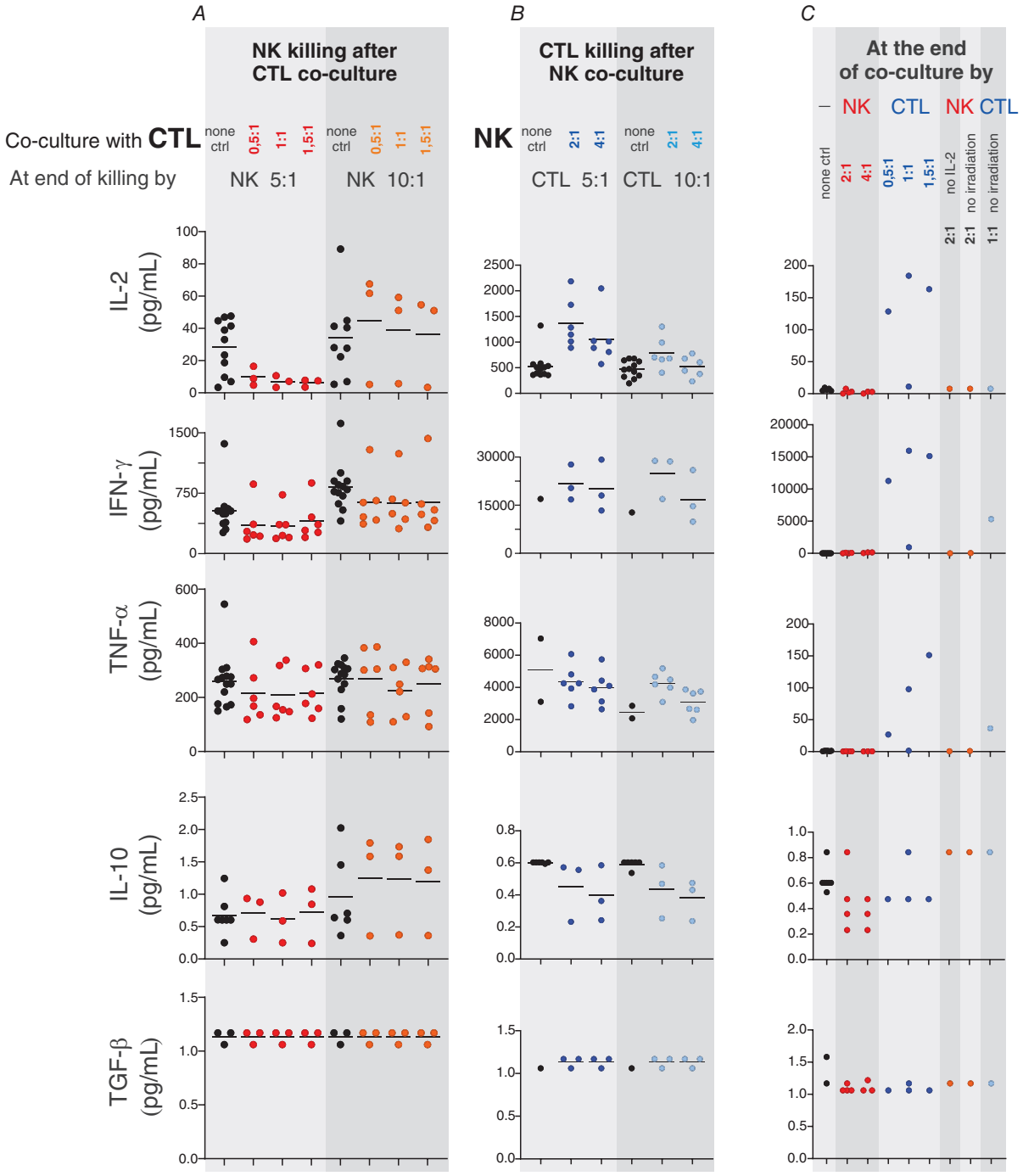

Figure 4. Cytokine and effector molecule detection assays to analyse the supernatant after cytotoxicity of fresh killer cells after pre-exposure or at the end of the initial pre-exposure
Supernatants were analysed with BD LEGENDplex. All concentrations are given in picograms per millilitre. *A* and *D*, SK-Mel-5 cells were co-cultured with different cytotoxic T lymphocytes-MART-1 clone 3 (CTL-M3)-to-SK-Mel-5 ratios as indicated. After this pre-exposure, surviving SK-Mel-5 cells were used in a cytotoxicity assay with fresh natural killer (NK) cells at effector-to-target (E:T) ratios of 5:1 or 10:1. The supernatant was collected immediately after 4 h. Signals for transforming growth factor-β (TGF-β) and partly also for interleukin-10 (IL-10) were mostly below the detection limit, which is the reason that values are identical (reflecting the detection limit). *B* and *E*, SK-Mel-5 cells were co-cultured with different NK cell-to-SK-Mel-5 cell ratios as indicated. After this pre-exposure, surviving SK-Mel-5 cells were used in a cytotoxicity assay with fresh CTL-M3 at E:T ratios of 5:1 or 10:1. The supernatant was collected immediately after 4 h. *C* and *F*, SK-Mel-5 cells were co-cultured with different NK cell or CTL-M3 ratios as indicated. Supernatants were collected after 3 days of co-culture with different effector cell conditions [with interleukin-2 (IL-2) and irradiation if not indicated otherwise].

Despite clear trends of reduced NK cell cytotoxicity against pre-exposed SK-Mel-5 cells, the analysis did not reach statistical significance in most cases. We therefore retested the effect with another experimental approach using SK-Mel-5 cells from a different supplier [SK-Mel-5(B) cells with lower MART-1 expression] at NK:SK-Mel-5 ratios between 2:1 and 10:1 during NK cell pre-exposure (Fig. 5*K*–*N*). Although these SK-Mel-5 cells were killed by NK cells less efficiently (Fig. 5*K*), the reduction of cytotoxic efficiency of fresh NK cells after pre-exposure was similar (Fig. 5*K*–*N*), and statistical significance was reached in many cases. In addition, the impairment in cytotoxicity of fresh NK cells against surviving SK-Mel-5 cells following NK cell pre-exposure was identical for both data sets (Fig. 5*E*). Considering the clear trends and statistical significance in many cases, we conclude that pre-exposure to low numbers of NK cells induces resistance of SK-Mel-5 cells against a subsequent exposure to fresh NK cells. It is very unlikely that resistant SK-Mel-5 cells pre-existed in the original culture, because all SK-Mel-5 cells were killed by sufficiently high numbers of CTL-M3 or NK cells (Fig. 2). We conclude

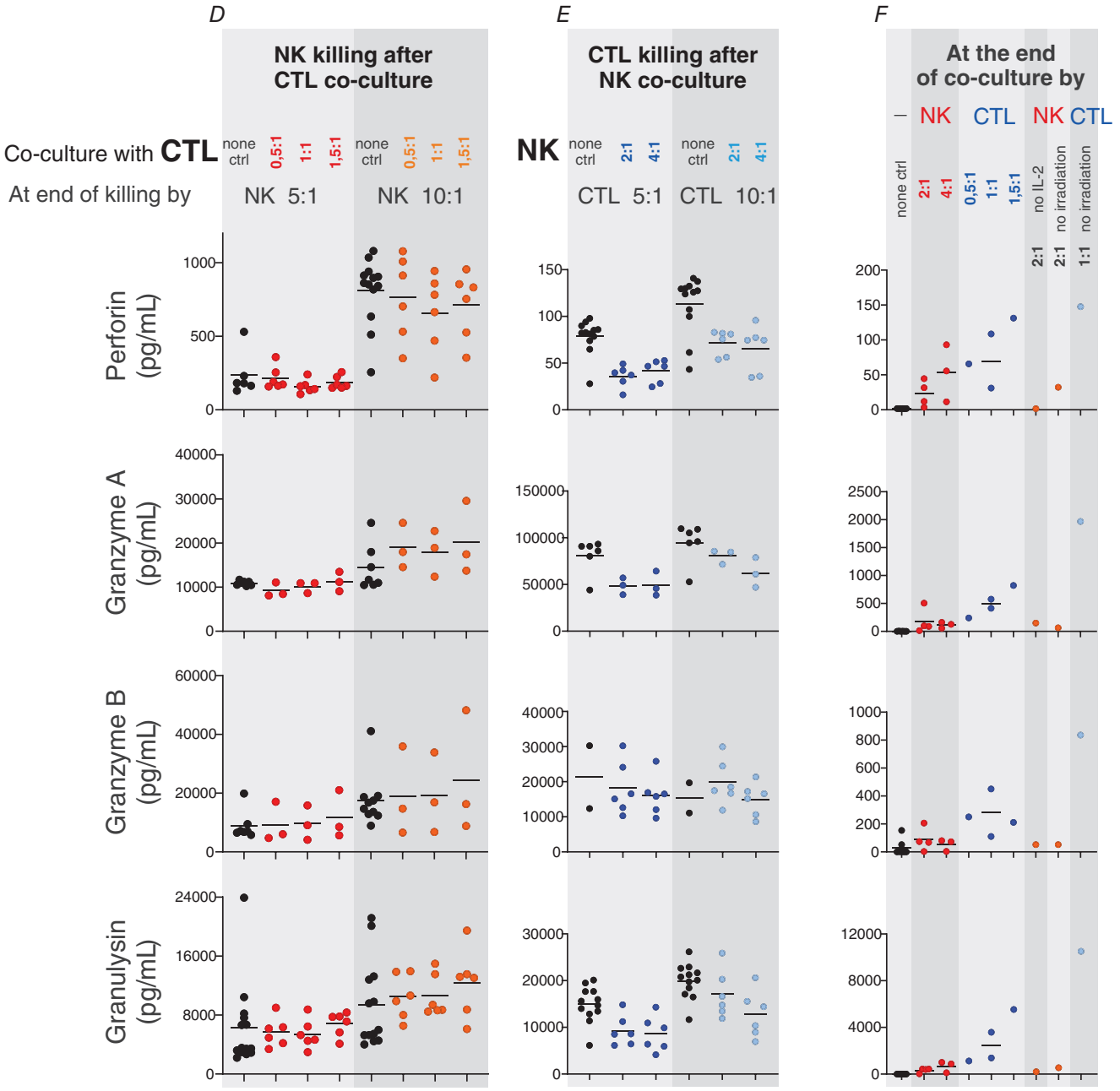

Figure 4. Continued

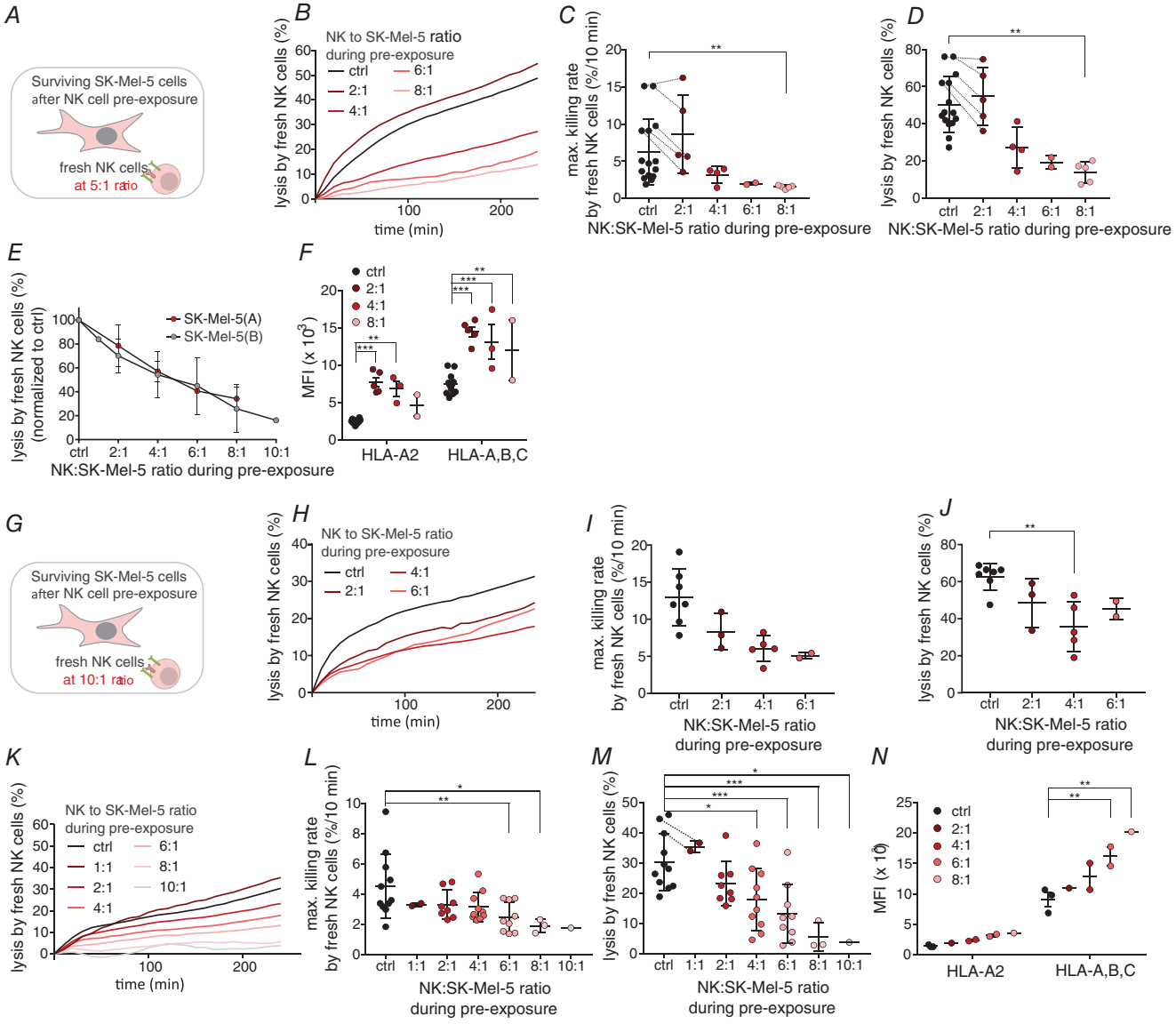

Figure 5. Natural killer cell–SK-Mel-5 cell pre-exposure induces resistance of surviving SK-Mel-5 cells against natural killer cell-mediated cytotoxicity

A and *B*, SK-Mel-5 cells were co-cultured for 3–4 days together with primary natural killer (NK) cells (*A*) at different NK cell-to-SK-Mel-5 cell (NK:SK-Mel-5) ratios as indicated in *B*. *B*, NK cell-mediated cytotoxicity was tested against surviving SK-Mel-5 cells at a fixed NK:SK-Mel-5 ratio of 5:1 following different NK:SK-Mel-5 cell pre-exposure ratios. *C* and *D*, maximal killing rate (*C*) and endpoint lysis after 240 min (*D*) were analysed to quantify NK cell cytotoxicity (n = 2–15). *E*, normalized NK cell cytotoxicity against SK-Mel-5 cells is compared between the data sets shown in *D* [SK-Mel-5(A) from ATCC] and *M* [SK-Mel-5(B) from CSL]. Relative target cell lysis (normalized to killing with no NK cells present during pre-exposure) is displayed against the respective NK:SK-Mel-5 pre-exposure ratio. *F*, human leucocyte antigen (HLA)-A2 and HLA-A, -B and -C expression of SK-Mel-5 cells pre-exposed at different NK:SK-Mel-5 ratios were analysed by flow cytometry (n = 2–12). *G–J*, independent confirmation that NK cell–SK-Mel-5 cell pre-exposure induces resistance against NK cell-mediated cytotoxicity. *G*, same as *A*, except that fresh NK cells were used at a ratio of 10:1. The SK-Mel-5 cells were pre-exposed for 3–4 days to NK cells at different NK:SK-Mel-5 ratios as indicated in *H*. *H*, NK cell-mediated cytotoxicity, which was tested against surviving SK-Mel-5 cells at an NK:SK-Mel-5 ratio of 10:1. *I* and *J*, maximal killing rate (*I*) and endpoint lysis after 240 min (*J*) were analysed to quantify NK cell cytotoxicity (n = 2–7). *K–N*, second independent confirmation that NK cell–SK-Mel-5 cell pre-exposure induces resistance against NK cell-mediated cytotoxicity. SK-Mel-5 cells from another supplier [CLS; SK-Mel-5(B)] were pre-exposed for 3–4 days to NK cells at different NK:SK-Mel-5 ratios (shown in *K*). *K*, NK cell-mediated cytotoxicity against surviving SK-Mel-5 cells at an NK:SK-Mel-5 ratio of 5:1. *L* and *M*, maximal killing rate (*L*) and endpoint lysis after 240 min (*M*) were analysed to quantify NK cell-mediated cytotoxicity (n = 1–11). *N*, HLA-A2 and HLA-A, -B and -C expression of SK-Mel-5 cells pre-exposed to different numbers of NK cells were analysed with flow cytometry (n = 1–3).

that pre-exposure of NK cells results in the survival of SK-Mel-5 cells, which acquire resistance to the cytotoxicity of freshly applied NK cells, similar to the findings of Balsamo et al. (2012). This effect is independent of the level of MART-1 expression, because it is similar for two different SK-Mel-5 cell lines with different MART-1 expression levels (compare Fig. 3*I–K*).

One reason for this resistance of surviving SK-Mel-5 cells to the cytotoxicity of fresh NK cells might be the upregulation of HLA class I molecules, which are well known to act as strong inhibitory ligands for NK cell cytotoxicity (Balsamo et al., 2012; Huergo-Zapico et al., 2018; Orr & Lanier, 2010). Their upregulation has been shown following IFN-γ release by killer cells (Derre et al., 2006; Malmberg et al., 2002). We therefore tested HLA class I expression and, as expected, found upregulation of HLA-A2 and HLA-A, -B and -C in SK-Mel-5 cells incubated with NK cells (Fig. 5*F* and *N*). We conclude that co-culture of NK cells and SK-Mel-5 cells reduces subsequent cytotoxic efficiency by fresh NK cells and that this effect could, in principle, be explained by upregulation of HLA class I in SK-Mel-5 cells.

We next tested the cytotoxicity of CTL-M3 against surviving SK-Mel-5 cells [at a 10:1 CTL-M3-to-SK-Mel-5 cell (CTL-M3:SK-Mel-5) ratio] after pre-exposure to NK cells (Fig. 6*A*). Figure 6*B* shows that cytotoxicity of CTL-M3 was not reduced after NK cell pre-exposure at NK:SK-Mel-5 E:T ratios between 2:1 and 6:1 during the co-culture compared with control. In contrast to all other combinations, there was an enhancement of CTL-M3 cytotoxic efficiency after co-culture of NK cells and SK-Mel-5 cells (Fig. 6*B*), which is also evident from the analysis of the maximal killing rate (Fig. 6*C*) and the target cell lysis at 240 min (Fig. 6*D*). This tendency was confirmed at an CTL-M3:SK-Mel-5 ratio of 5:1 (Fig. 6*E–H*) and was significant for the maximal killing rate (Fig. 6*G*). In conclusion, cytotoxic efficiency after NK cell pre-exposure during co-culture is reduced for fresh NK cells but, on the contrary, enhanced for CTL-M3 against surviving SK-Mel-5 cells.

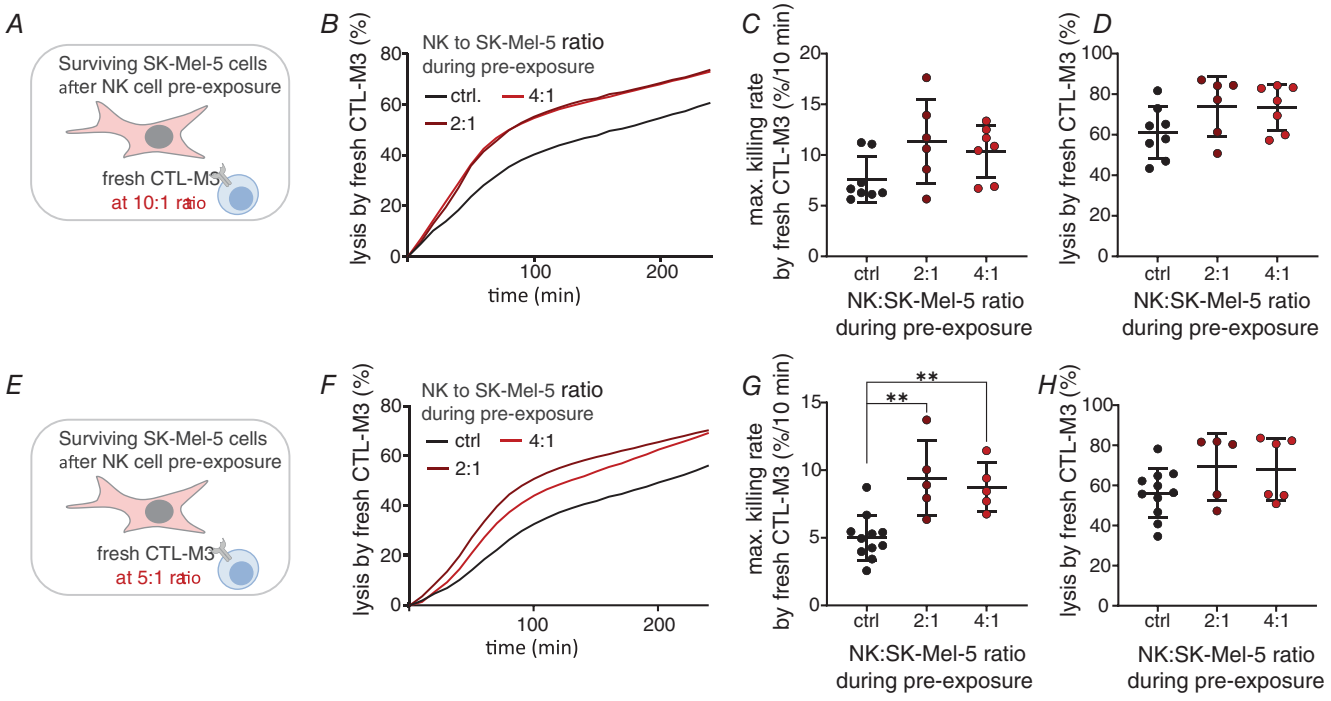

Figure 6. Natural killer cell–SK-Mel-5 cell pre-exposure increases cytotoxicity mediated by cytotoxic T lymphocytes-MART-1 clone 3 against surviving SK-Mel-5 cells
A and *B*, SK-Mel-5 cells were co-cultured for 3–4 days with primary natural killer (NK) cells (*A*) at different NK cell-to-SK-Mel-5 cell (NK:SK-Mel-5) ratios (*B*). *B*, cytotoxic T lymphocytes-MART-1 clone 3 (CTL-M3)-mediated cytotoxicity against surviving SK-Mel-5 cells at a fixed 10:1 effector-to-target (E:T) ratio following pre-exposure to NK cells at different ratios during co-culture. *C* and *D*, maximal killing rate (*C*) and endpoint lysis after 240 min (*D*) were analysed to quantify CTL-M3-mediated cytotoxicity (n = 1–7). *E–H*, independent confirmation that NK cell–SK-Mel-5 cell pre-exposure does not induce resistance against CTL-M3-mediated cytotoxicity. *E*, same as *A*, except that fresh CTL-M3 were used at a ratio of 5:1. *F*, SK-Mel-5 cells were pre-exposed for 3–4 days to NK cells at different NK:SK-Mel-5 ratios; CTL-M3-mediated cytotoxicity was assessed against surviving SK-Mel-5 cells at a 5:1 E:T ratio. *G* and *H*, maximal killing rate (*G*) and endpoint lysis after 240 min (*H*) were analysed to quantify CTL-M3-mediated cytotoxicity (n = 1–10).

Cytotoxic efficiency of NK cells and CTL-M3 against melanoma cells surviving CTL pre-exposure

To examine the potential interdependence of NK cell and CTL-M3 cytotoxic efficiency further, we reversed the approach and pre-exposed SK-Mel-5 melanoma cells at different CTL-M3:SK-Mel-5 ratios between 0.5:1 and 2:1 (Fig. 7*A*) and tested the cytotoxicity of fresh CTL-M3 or NK cells after CTL-M3 pre-exposure (Figs 7 and 8). A pre-exposure ratio between 0.5:1 and 2:1 was chosen

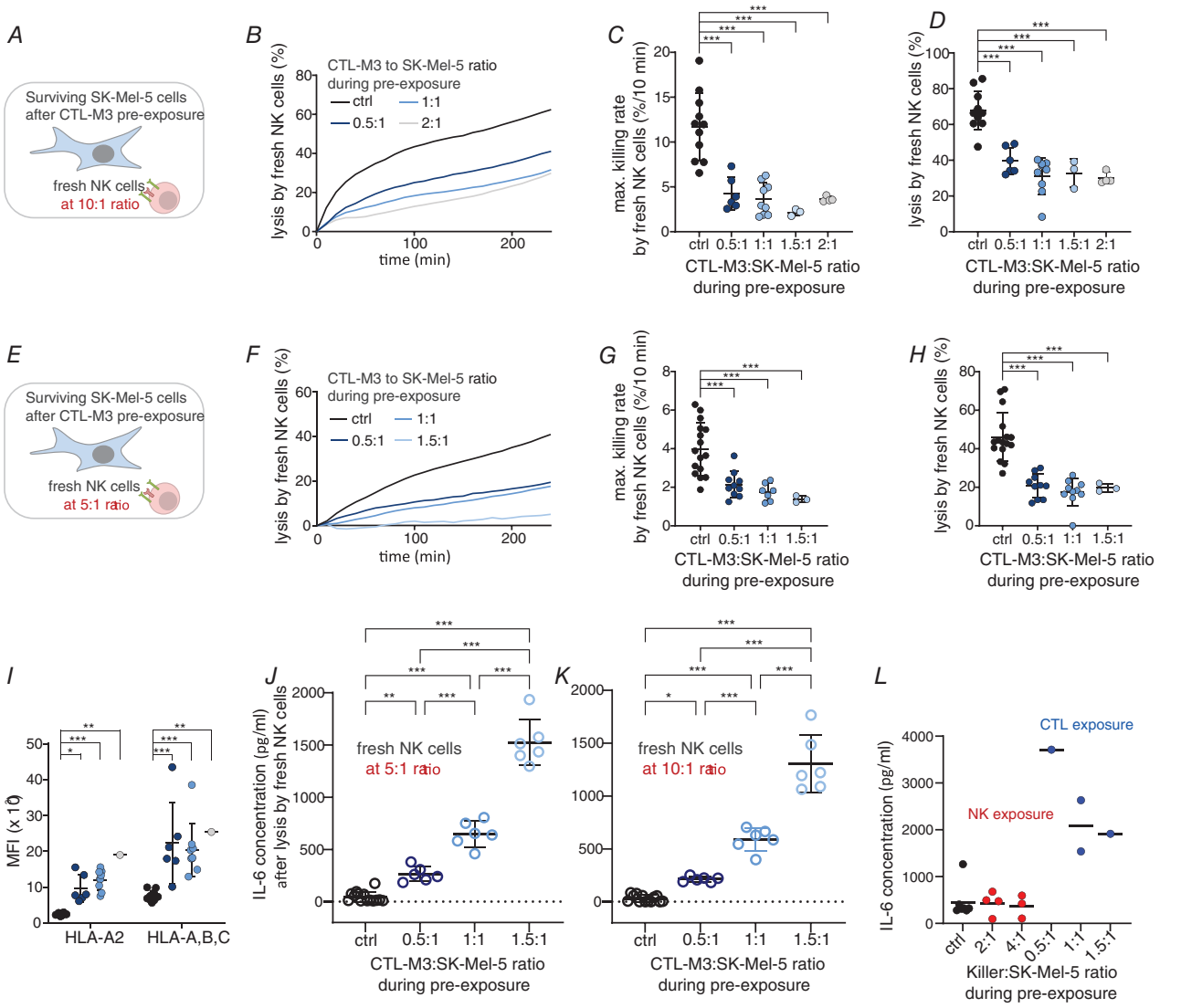

Figure 7. Cytotoxic T lymphocyte-M3–SK-Mel-5 cell pre-exposure induces resistance of surviving SK-Mel-5 cells against natural killer cell-mediated cytotoxicity
A and *B*, SK-Mel-5 cells were pre-exposed for 3–4 days to cytotoxic T lymphocytes-MART-1 clone 3 (CTL-M3) (*A*) at different CTL-M3-to-SK-Mel-5 cell (CTL-M3:SK-Mel-5) ratios (*B*). *B*, NK cell-mediated cytotoxicity against surviving SK-Mel-5 pre-exposed to CTL-M3, tested at a fixed NK cell-to-SK-Mel-5 cell ratio of 10:1 after different CTL-M3:SK-Mel-5 pre-exposure ratios. *C* and *D*, maximal killing rate (*C*) and endpoint lysis after 240 min (*D*) were analysed to quantify NK cell-mediated cytotoxicity against SK-Mel-5 cells surviving pre-exposure (n = 3–8). *E–H*, independent confirmation that CTL-M3–SK-Mel-5 cell pre-exposure induces resistance against NK cell-mediated cytotoxicity. *E*, same as *A*, except that fresh NK cells were used at a ratio of 5:1. *F*, SK-Mel-5 cells were pre-exposed for 3–4 days to CTL-M3 at different CTL-M3:SK-Mel-5 ratios, and NK cell-mediated cytotoxicity was assessed against surviving SK-Mel-5 cells. *G* and *H*, maximal killing rate (*G*) and endpoint lysis after 240 min (*H*) were analysed to quantify NK cell-mediated cytotoxicity against surviving SK-Mel-5 cells (n = 2–13). *I*, human leucocyte antigen (HLA)-A2- and HLA-A, -B and -C expression of SK-Mel-5 cells pre-exposed to different numbers of CTL-M3 were analysed in flow cytometry (n = 1–12). *J* and *K*, determination of interleukin-6 (IL-6) concentration at the end of NK cell killing of SK-Mel-5 cells at a 5:1 (*J*) or 10:1 (*K*) ratio after CTL-M3 pre-exposure. *L*, IL-6 concentration in supernatants after 3 days of pre-exposure to no other cells (ctrl), NK cells or CTL-M3 at the ratios indicated.

because all SK-Mel-5 cells were eliminated at higher CTL-M3:SK-Mel-5 ratios during the co-culture.

Natural killer cell cytotoxicity against surviving SK-Mel-5 cells (at 10:1 NK:SK-Mel-5 ratio; Fig. 7*A*) following CTL-M3 pre-exposure was significantly reduced at very low CTL-M3:SK-Mel-5 ratios during pre-exposure (Fig. 7*B*), as quantified by the maximal killing rate (Fig. 7*C*) and the final lysis at 240 min (Fig. 7*D*). Independent experiments at 5:1 NK:SK-Mel-5 ratio confirmed that NK cytotoxicity after CTL-M3

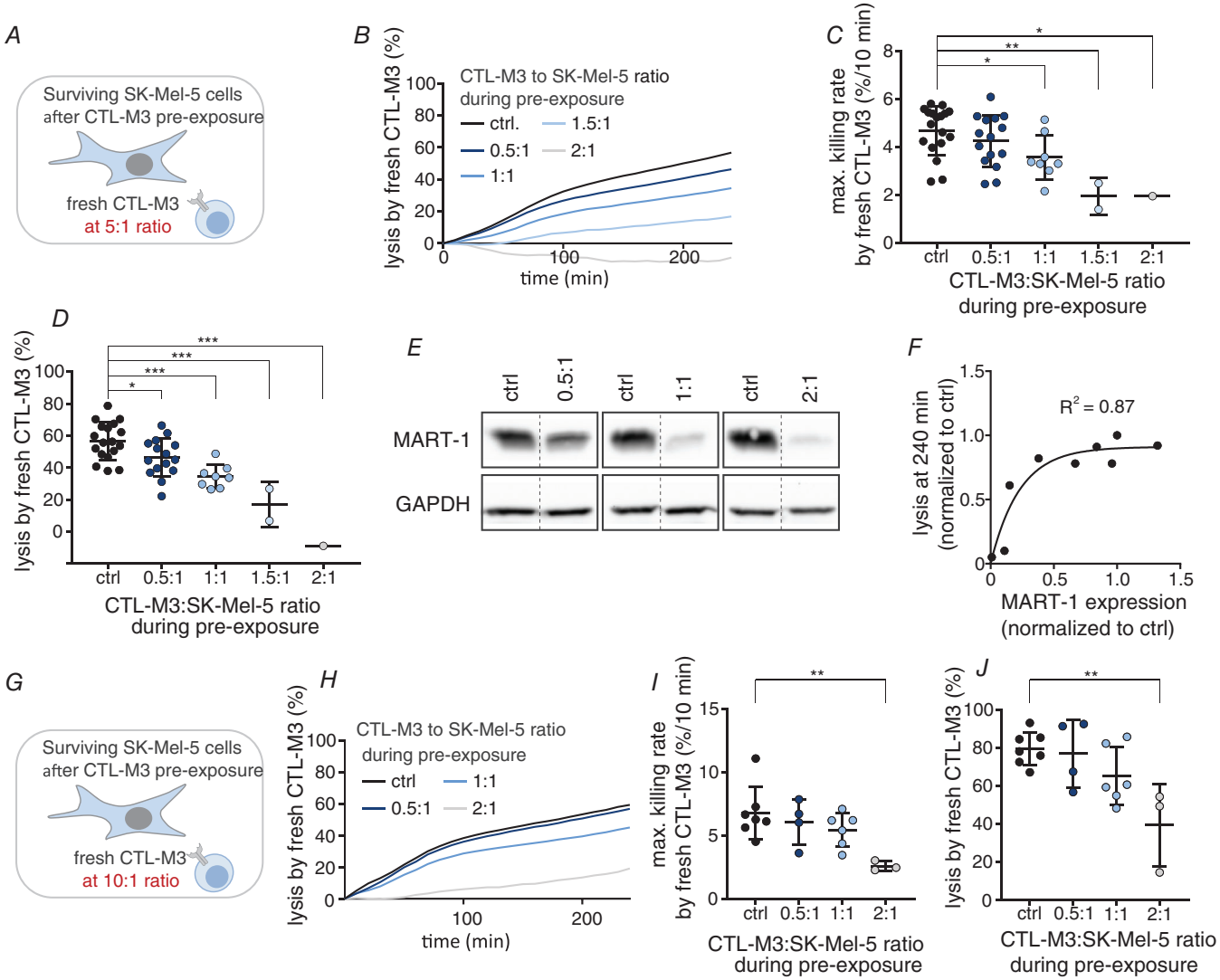

Figure 8. Cytotoxic T lymphocytes-MART-1 clone 3 (CTL-M3)–SK-Mel-5 cell pre-exposure induces resistance of surviving SK-Mel-5 cells against CTL-M3-mediated cytotoxicity
A and *B*, SK-Mel-5 cells were pre-exposed for 3–4 days to cytotoxic T lymphocytes-MART-1 clone 3 (CTL-M3) (*A*) at different CTL-M3-to-SK-Mel-5 cell (CTL-M3:SK-Mel-5) ratios (*B*). *B*, CTL-M3-mediated cytotoxicity against surviving SK-Mel-5 cells was tested at a fixed CTL-M3:SK-Mel-5 ratio of 5:1 after different CTL-M3:SK-Mel-5 pre-exposure ratios. *C* and *D*, maximal killing rate (*C*) and endpoint lysis after 240 min (*D*) were analysed to quantify CTL-M3-mediated cytotoxicity against surviving SK-Mel-5 cells (n = 1–18). *E*, western blots of SK-Mel-5 MART-1 expression after different CTL-M3–SK-Mel-5 cell pre-exposure conditions compared wth control conditions (no CTL-M3 during pre-exposure). The full blots are shown in Fig. 9, with the respective conditions shown in *E* marked in red. The dotted lines indicate that the bands were not juxtaposed on the blot, but they were always from the same blot. *F*, correlation of SK-Mel-5 lysis as measured in *B* and *D* against the respective amount of MART-1 protein as measured in *E* or in Fig. 9. *G–J*, independent confirmation that CTL-M3–SK-Mel-5 cell pre-exposure induces resistance against CTL-M3-mediated cytotoxicity. *G*, same as *A*, except that fresh CTL-M3 were used at a ratio of 10:1. *G* and *H*, SK-Mel-5 cells were pre-exposed for 3–4 days to CTL-M3 (*G*) at different CTL-M3:SK-Mel-5 ratios (*H*). *H*, CTL-M3-mediated cytotoxicity against surviving SK-Mel-5 cells. *I* and *J*, maximal killing rate (*I*) and endpoint lysis after 240 min (*J*) were analysed to quantify CTL-M3-mediated cytotoxicity against surviving SK-Mel-5 cells (n = 3–7).

pre-exposure was reduced (Fig. 7*E*–*H*). Pre-exposure of SK-Mel-5 cells to CTL-M3 clearly increased HLA class I expression (Fig. 7*I*), similar to the observations following pre-exposure to NK cells and SK-Mel-5 cells (compare Fig. 5*F* and *N*). Increased HLA class I expression on SK-Mel-5 cells is correlated with reduced NK cell cytotoxicity and could thus explain this reduction after CTL-M3 pre-exposure.

However, there are other possibilities. One possibility is that resistant SK-Mel-5 cells pre-exist in the culture and that these outnumbered the non-resistant cells after many of those were killed. We believe that this is, however, very unlikely for the following two reasons. First, in Fig. 2, we showed that high NK:SK-Mel-5 or CTL-M3:SK-Mel-5 ratios eliminate all melanoma cells. Thus, we conclude that there are no resistant SK-Mel-5 cells *per se* in the co-culture. Second, if we assume, for example, that 1% of SK-Mel-5 cells are resistant to CTL-M3 or NK cells, the initially 10^4 resistant cells (out of 10^6 SK-Mel-5 cells) would proliferate by a factor of 3.4 (Fig. 3*E*) to 3.4×10^4 cells. Compared with 0.97×10^6 cells surviving when CTL-M3 were used at a 1:1 ratio (Fig. 3*E*), this number is negligible and cannot explain the reduced killing capacity NK cells after CTL-M3 pre-exposure.

Cytokines control the immune responses in many ways. We did not detect correlations between the reduced killing efficiency and cytokine levels of IL-2, IFN-γ, TNF-α, IL-10 and TGF-β (Fig. 4*A*–*C*), all of which can be produced by CTL and NK cells and affect their functioning (Ochayon & Waggoner, 2021). Also, changes in perforin, granzyme A, granzyme B and granulysin levels released from CTL-M3 or NK-cells are not correlated with the reduced NK killing efficiency (Fig. 4*D*–*F*).

Besides the cytokines tested so far, the I-L6 family of cytokines plays a prominent role in the interaction of immune cells and cancer (Jones & Jenkins, 2018). Low concentrations of the founding member, IL-6, are reported to be beneficial for the immune response against cancer, whereas pathophysiological consequences of high magnitudes or durations of IL-6 exposure appear to be correlated with poor clinical outcomes in cancer in general (Jones & Jenkins, 2018) and in melanoma (Kucera et al., 2015). Considering these data, we tested IL-6 levels during NK cell killing of melanoma cells after CTL-M3 exposure. We found that IL-6 levels were increased after NK cell killing of surviving SK-Mel-5 cells that had been pre-exposed to increasing numbers of CTL-M3 at both 5:1 and 10:1 ratios (Fig. 7*J* and *K*). The more CTL-M3 were used during pre-exposure, the higher the IL-6 levels were after the NK killing of survivors. There was no difference between 5:1 or 10:1 NK cell to surviving SK-Mel-5 cell ratios, which indicates that the source of IL-6 is SK-Mel-5 cells (or CTL-M3) rather than the NK cells, because it is well known that tumour cells, including melanoma cells, produce IL-6. In addition, we did not find any IL-6 production after the first NK cell encounter during the co-culture with NK cells and SK-Mel-5 cells (Fig. 7*L*) but after the first CTL-M3 encounter during the co-culture of CTL-M3 and SK-Mel-5 cells (Fig. 7*L*). We conclude that, in addition to increased HLA expression, IL-6 levels are correlated with the inhibition of NK cell killing efficiency.

Focusing on the increased HLA class I expression on surviving SK-Mel-5 cells following CTL-M3 pre-exposure, we predicted that fresh CTL-M3 should eliminate surviving SK-Mel-5 cells more efficiently after CTL-M3–SK-Mel-5 cell pre-exposure (Fig. 8*A*). We tested this prediction by applying fresh CTL-M3 at an CTL-M3:SK-Mel-5 ratio of 5:1 after CTL-M3–SK-Mel-5 cell pre-exposure (Fig. 8*A* and *B*). However, to our surprise, cytotoxicity of fresh CTL-M3 was significantly reduced (Fig. 8*B*), as quantified by the maximal killing rate (Fig. 8*C*) and the endpoint target lysis at 240 min (Fig. 8*D*). Independent experiments at a 10:1 CTL-M3:SK-Mel-5 ratio confirmed that cytotoxicity after pre-exposure with CTL-M3 was reduced (Fig. 8*G*–*J*).

Given that expression of HLA-A2 and HLA-A, -B and -C was increased on SK-Mel-5 cells (compare Fig. 7*I*) following CTL-M3 pre-exposure, reduced HLA class I expression was eliminated as a potential cause for reduced cytotoxicity of fresh CTL-M3 against surviving SK-Mel-5 cells.

Another potential explanation for the reduced cytotoxic efficiency of fresh CTL-M3 against SK-Mel-5 cells pre-exposed to CTL-M3 could be a reduction of MART-1 antigen expression or reduced presentation on surviving SK-Mel-5 cells. To test whether reduced MART-1 expression of surviving SK-Mel-5 cells accounted for reduced CTL-M3 cytotoxic efficiency after CTL-M3–SK-Mel-5 cell pre-exposure, we tested MART-1 protein expression on SK-Mel-5 cells by western blot. We found that MART-1 expression on surviving SK-Mel-5 cells was reduced after CTL-M3 pre-exposure compared with the control (Fig. 8*E*). Quantification of all western blot conditions, shown in Fig. 9, revealed a correlation between MART-1 expression of surviving SK-Mel-5 cells and CTL-M3 cytotoxicity against these SK-Mel-5 cells (Fig. 8*F*). In comparison to the strong effect on MART-1 expression of CTL-M3 pre-exposure, NK cell pre-exposure reduced MART-1 expression to only a modest extent at high E:T ratios (Fig. 9). This finding is in line with the finding that CTL-M3 cytotoxicity against surviving SK-Mel-5 cells was not reduced but was even enhanced after NK cell pre-exposure (Fig. 6).

Considering these results, it is likely that reduction of MART-1 expression is responsible for reduced CTL-M3 cytotoxicity against surviving SK-Mel-5 cells after CTL-M3 pre-exposure. To test this hypothesis, we designed a rescue experiment by loading external MART-$1_{26–35A27L}$ peptide on the surviving SK-Mel-5 cells. Figure 10*A* illustrates the settings of the rescue

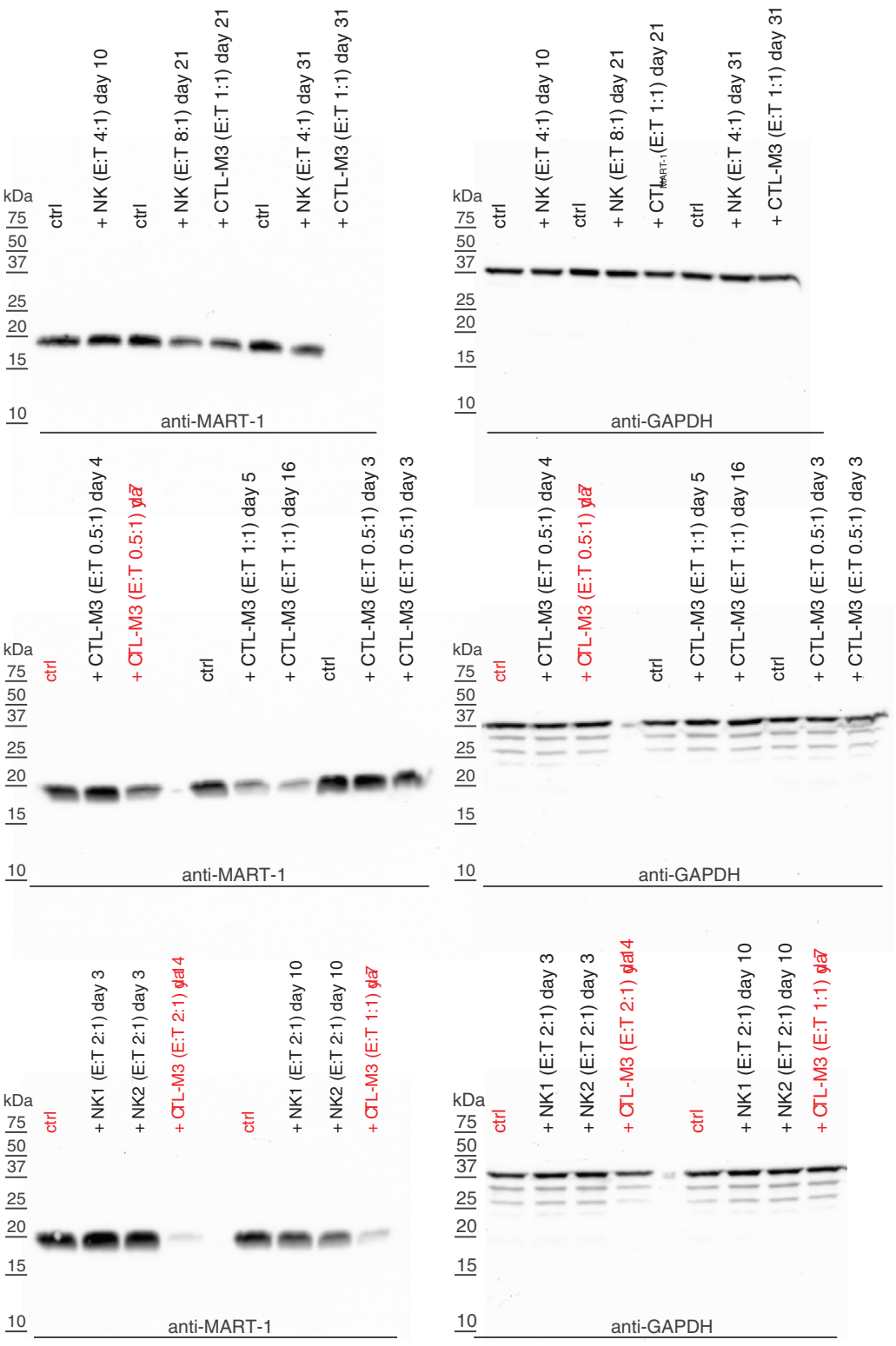

Figure 9. Cytotoxic T lymphocyte–M3-SK-Mel-5 cell pre-exposure induces downregulation of MART-1 protein expression on SK-Mel-5 cells
Complete western blots used in Fig. 8*E* and *F*. SK-Mel-5 cells were pre-exposed to cytotoxic T lymphocytes-MART-1 clone 3 (CTL-M3) or natural killer (NK) cells at different effector-to-target (E:T) ratios. Indicated in red are the samples shown in Fig. 8*E*.

experiment. Pre-exposure of CTL-M3 increased HLA-A2 and HLA-A, -B, -C expression on SK-Mel-5 cells (compare Fig. 7*I*) but decreased MART-1 expression (Fig. 8*E*). Considering this finding, it makes sense that fresh CTL-M3 show reduced cytotoxicity against surviving SK-Mel-5 cells (Fig. 8*B*–*D*). This should be rescued by exogenous MART-1 antigen. We found that additional loading with MART-1 antigen on surviving SK-Mel-5 cells (Fig. 10*A*, right panel) was indeed sufficient to rescue CTL-M3 cytotoxicity against surviving SK-Mel-5 cells (Fig. 10*B*) as quantified by the maximal killing rates (Fig. 10*C*) and the endpoint lysis at 240 min (Fig. 10*D*).

The rescue experiments even induced more efficient CTL-M3 cytotoxicity compared with control conditions, which can be explained by the increased HLA-A2 expression on SK-Mel-5 cells following CTL-M3 pre-exposure and thus an increased MART-1 presentation on the surface of surviving SK-Mel-5 after peptide loading.

We conclude that decreased MART-1 antigen expression on surviving SK-Mel-5 cells after pre-exposure to CTL-M3 is causative of the reduced CTL-M3 cytotoxicity against the surviving SK-Mel-5 melanoma cells. Furthermore, enhanced HLA-A2 expression on surviving SK-Mel-5 cells after CTL-M3 pre-exposure increases CTL-M3 cytotoxicity against surviving SK-Mel-5 cells beyond control levels if, additionally, exogenous MART-1 antigen is provided.

Discussion

Although it is common knowledge that cancer cells can evade the immune system, very few publications have addressed the quantification of CTL or NK cell cytotoxicity directly. Balsamo et al. (2012) showed that melanoma cells acquired a protective phenotype against human NK cells during long-term co-cultures with low numbers of NK cells as reported in tumours. Expression of HLA class I was increased in melanoma cells when insufficient numbers of NK cells were present to eradicate all melanoma cells (Balsamo et al., 2012; Huergo-Zapico et al., 2018). Kohlhapp et al. (2015) and Xu et al. (2004) analysed the roles of murine CTL and NK cells, showing that both cytotoxic cell types are involved in

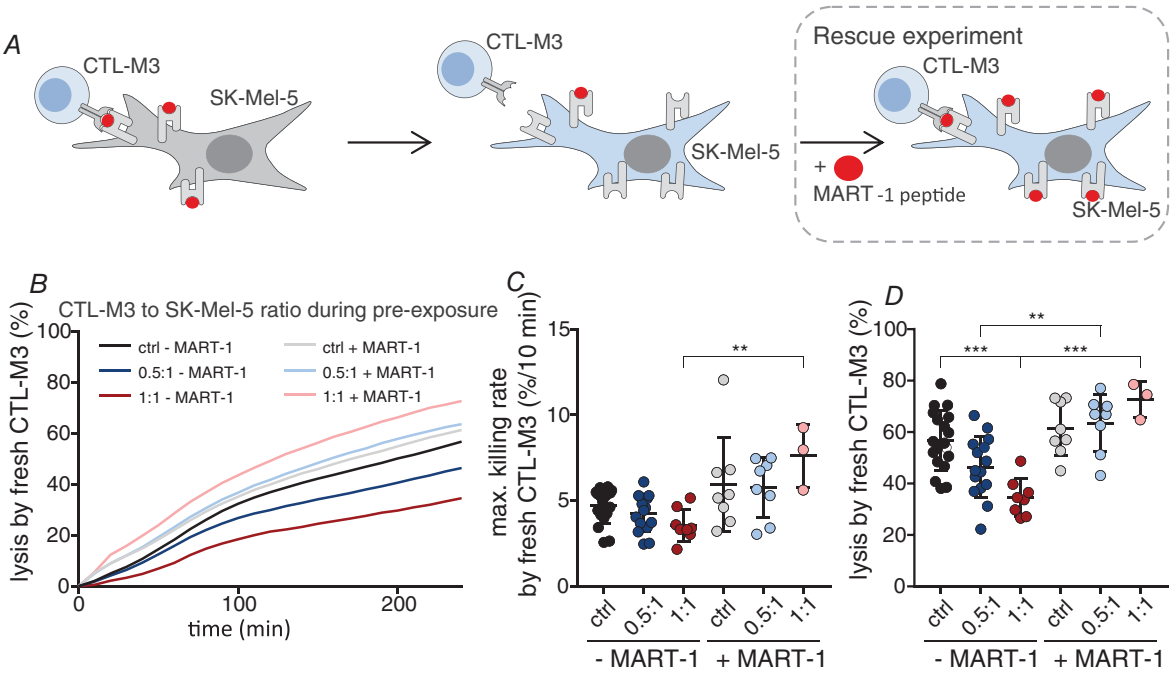

Figure 10. Susceptibility to cytotoxic T lymphocytes-MART-1 clone cytotoxicity can be rescued by loading the surviving SK-Mel-5 cells with exogenous MART-1 peptide
A, schematic representation of the experimental set-up. SK-Mel-5 cells surviving cytotoxic T lymphocytes-MART-1 clone 3 (CTL-M3) pre-exposure acquire resistance against CTL-M3 cytotoxicity by lowering MART-1 antigen expression while upregulating human leucocyte antigen (HLA) class I molecules. The rescue strategy, by exogenous loading of MART-1 antigen on SK-Mel-5 cells surviving CTL-M3 pre-exposure, is illustrated. *B*, CTL-M3-mediated cytotoxicity against SK-Mel-5 cells at a fixed CTL-M3-to-SK-Mel-5 cell (CTL-M3:SK-Mel-5) ratio of 5:1 measured after CTL-M3–SK-Mel-5 cell pre-exposure, with (+MART-1) or without (−MART-1) exogenous peptide loading. Control SK-Mel-5 cells (no co-culture with CTL-M3) were also included in the measurement. *C* and *D*, maximal killing rate (*C*) and endpoint lysis after 240 min (*D*) were analysed to quantify CTL-M3-mediated cytotoxicity (n = 3–18).

the eradication of melanoma, and Le et al. (2020) found that both CTL and NK cells are important for control of solid tumours in a novel patient-derived xenograft model. Neubert et al. (2016) developed a well-controlled co-culture assay for human melanoma and CTL to analyse future T cell-based immunotherapies. None of these studies, however, was focused on whether and how CTL and NK cells influence each other's cytotoxicity. The reason for this might be the technical complexity. Thus, an assay is needed to quantify sequential antigen-dependent CTL and NK cell cytotoxicity.

The assay we developed here allows exactly this, by analysing MART-1-specific human CTL and NK cell cytotoxicity using the same melanoma cell targets. In addition, this *in vitro* assay with primary human cells could also provide a platform to replace or reduce *in vivo* murine experiments in line with '3R' concepts.

As proof of principle for our assay, we first confirmed the finding that pre-exposure of melanoma cells to insufficient numbers of NK cells renders surviving melanoma cells less susceptible to further NK cell cytotoxicity (Balsamo et al., 2012; Huergo-Zapico et al., 2018). Making use of our assay, we then tested all combinations. We found that NK cell cytotoxicity after pre-exposure of melanoma cells to either CTL or NK cells was reduced, as was CTL cytotoxicity after CTL pre-exposure. In all three conditions, pre-exposure induced resistance in surviving melanoma cells. Resistance was higher if high E:T ratios of CTL or NK cells to melanoma cells were used during pre-exposure. This means that if not eradicated completely, a higher number of CTL or NK cells induces a higher degree of resistance in the surviving melanoma cells. Interestingly, a recent computational model predicts that it is beneficial for controlling tumour growth to apply lower numbers of CTL several times rather than the equivalent number of cells only once (Khazen et al., 2019). In support of a recurrent therapy with low numbers of CTL, we found that CTL-M3 have a good cytotoxic potential at low antigen concentration, which fits well with the important finding that T cells can be activated by very few antigen–MHC contacts (Huang et al., 2013). In principle, each antigen-specific CTL should be able to kill even if little antigen is presented. To optimize the perfect dose of CTL for immunotherapy, kinetic information on individual CTL would be helpful, which is something that microscopy assays can provide.

Is it possible to distinguish whether melanoma cells with pre-existing resistance were selected or if resistance was induced? Our finding that all melanoma cells can be eliminated by large numbers of CTL or NK cells strongly suggests that pre-exposure induces resistance of melanoma cells rather than selecting melanoma cells with pre-existing resistance. Melanoma, although not an epithelial cancer, can also undergo an epithelial-to-mesenchymal transition (EMT)-like transition towards mesenchymal traits. Epithelial-to-mesenchymal transition has been implicated in carcinogenesis and metastasis of various cancers (Mittal, 2018) and can be induced in melanoma cell lines by NK cell editing (Huergo-Zapico et al., 2018). It can be elicited within hours (Miettinen et al., 1994) or days (Huergo-Zapico et al., 2018), thus certainly in $<$3–4 days, which was the pre-exposure time in our culture. Phenotype switching, however, can occur not only by EMT mechanisms and might involve common switch inducers (via EMT or other mechanisms), such as transcription factors including SNAIls, ZEBs, TWIST or c-Jun, but also the melanocytic lineage marker MITF (microphthalmia-associated transcription factor) or beta-catenin interaction factors LEF1 and TCF4 (Li et al., 2015; Mittal, 2018). Signalling pathways responsible for EMT include Wnt, Notch and TGF-β (Dongre & Weinberg, 2019). Although phenotype switching can facilitate metastasis, migration and invasion, it is not clear whether it always induces melanoma cell resistance to CTL or NK cells. Only few of the numerous associated changes in gene expression have been related to melanoma resistance. Among others, melanoma cells have been shown to protect themselves by decreasing the anti-tumour activity of NK cells through inhibition of NK cell-activating receptors, such as NKG2D (Pietra et al., 2012), or by neutralizing CTL cytotoxicity through increased lysosome secretion (Khazen et al., 2016). Neither of these mechanisms explains our phenotypes, because we expose the surviving melanoma cells to fresh CTL or NK cells.

Among the most relevant ligands modulating CTL and NK cell cytotoxicity against cancer, HLA class I molecules on cancer cells have a distinguished role because of their dual function. They are required for CTL cytotoxicity but inhibit NK cell cytotoxicity. An increase of HLA expression was reported following IFN-γ release by killer cells (Derre et al., 2006; Malmberg et al., 2002). Expression of HLA class I receptor was indeed increased after co-culture of melanoma and NK cells, and this is considered a main route to induce melanoma resistance to NK cell cytotoxicity (Balsamo et al., 2012; Huergo-Zapico et al., 2018).

In addition, CTL pre-exposure also enhanced HLA-A2 and HLA-A, -B and -C expression, which can explain the reduced NK cell cytotoxicity against melanoma cells surviving either CTL or NK cell pre-exposure. Upregulation of HLA was correlated with decreased NK cytotoxicity, pointing to a higher resistance of surviving melanoma cells exposed to high numbers of CTL or NK cells.

This finding again favours the computational model prediction to apply lower numbers of CTL several times rather than the equivalent number of cells once (Khazen et al., 2019). Increased HLA-A2 and HLA-A, -B and -C

expression can also explain why CTL cytotoxicity against surviving melanoma was not reduced but was even slightly enhanced after NK cell pre-exposure. It could be beneficial to combine NK cell and CTL immunotherapy, but only if started with NK cells.

Although increased HLA-A2 and HLA-A, -B and -C offers a good explanation for these three cases, it does not explain the effects of CTL pre-exposure on subsequent CTL cytotoxicity. Higher HLA-A2 and HLA-A, -B and -C expression after CTL pre-exposure should not inhibit cytotoxicity of fresh CTL against the surviving melanoma cells, but should increase it. Reduced CTL cytotoxicity against surviving melanoma cells following CTL pre-exposure is, however, explained by a fundamental difference between CTL and NK cell pre-exposure. Both increased HLA-A2 and HLA-A, -B and -C expression, but only CTL pre-exposure diminished the expression of MART-1 antigen at the same time. The loss of MART-1 antigen is the key factor, because adding MART-1 antigen to melanoma cells pre-exposed to CTL could completely rescue the subsequent cytotoxic efficiency of fresh CTL.

In addition to HLA upregulation, we found that IL-6 levels were correlated with the inhibition of NK cell killing efficiency. There is good evidence that high IL-6 levels are correlated with poor clinical outcomes in cancer, including melanoma (Jones & Jenkins, 2018; Kucera et al., 2015). Thus, IL-6 could be involved in reducing NK cell cytotoxic efficiency against SK-Mel-5 cells, but more experiments are needed to substantiate this and to gain a better understanding of the molecular mechanisms. Another potential mechanism to reduce NK cell cytotoxicity after CTL pre-exposure was published recently by Walwyn-Brown et al. (2022), who showed that $\gamma\delta$ T cells can suppress NK cell cytotoxicity stimulated by HLA-deficient targets. This reduction required direct contact, which can therefore not explain the effects observed here, because killer cell types were applied sequentially.

Quantification of CTL cytotoxicity has revealed differences between the *in vivo* and *in vitro* situations. Efficient cytotoxicity has been reported in *in vitro* settings (Mempel et al., 2006; Purbhoo et al., 2004), whereas cytotoxicity was found to be less efficient *in vivo* (Breart et al., 2008; Boissonnas et al., 2007; Engelhardt et al., 2012; Halle et al., 2016). Currently, the reason for this is not clear. Additive cytotoxicity of CTL has recently been shown to influence cytotoxic efficiency significantly (Weigelin et al., 2021). Our *in vitro* approach might add to the understanding of the differences in cytotoxic efficiency between *in vivo* and *in vitro* conditions. Although we find high cytotoxicity, as reported by others *in vitro*, we can also mimic drastically reduced cytotoxicity, as reported in the *in vivo* situation. Pre-exposure to CTL drastically reduces CTL cytotoxic efficiency. Cytotoxic T lymphocytes are usually present in persisting tumours, and we predict that their presence should contribute to low *in vivo* CTL cytotoxicity. Thus, *in vitro* and *in vivo* discrepancies can be reconciled by our findings.

To quantify kinetics of cancer cell eradication by combination of CTL and NK cells could therefore prove a helpful *in vitro* tool to test cytotoxic efficiencies and quantify the numbers of CTL and NK cells for immune therapy. Considering our results, we propose the following:

(1) If available and if control of side effects allows this, patients should be treated with a large number of CTL or NK cells, because only this guarantees the avoidance of escape mechanisms. This is a trivial result, and we are, of course, not the first ones to propose this.
(2) If it is not possible to eradicate the tumour at once with a high dose of CTL or NK cells, it might be beneficial to stimulate repeatedly with lower doses to avoid strong melanoma resistance, as has been suggested by Khazen et al. (2019) based on a computer model. Our experimental set-up might be well suited to determine the relevant time interval still to benefit from repeated treatment with low doses while avoiding induction of resistance to cytotoxicity.
(3) Antigen loss can be a severe complication during extended or repeated CTL therapies, and this should be considered during immune therapy.
(4) If possible, CTL immune treatment should be used after NK cell treatment, which is also the physiological order of events.

References

Backes, C. S., Friedmann, K. S., Mang, S., Knorck, A., Hoth, M., & Kummerow, C. (2018). Natural killer cells induce distinct modes of cancer cell death: Discrimination, quantification, and modulation of apoptosis, necrosis, and mixed forms. *The Journal of Biological Chemistry*, **293**(42), 16348–16363.

Balsamo, M., Vermi, W., Parodi, M., Pietra, G., Manzini, C., Queirolo, P., Lonardi, S., Augugliaro, R., Moretta, A., Facchetti, F., Moretta, L., Mingari, M. C., & Vitale, M. (2012). Melanoma cells become resistant to NK-cell-mediated killing when exposed to NK-cell numbers compatible with NK-cell infiltration in the tumor. *European Journal of Immunology*, **42**(7), 1833–1842.

Barry, K. C., Hsu, J., Broz, M. L., Cueto, F. J., Binnewies, M., Combes, A. J., Nelson, A. E., Loo, K., Kumar, R., Rosenblum, M. D., Alvarado, M. D., Wolf, D. M., Bogunovic, D., Bhardwaj, N., Daud, A. I., Ha, P. K., Ryan, W. R., Pollack, J. L., Samad, B., … Krummel, M. F. (2018). A natural killer-dendritic cell axis defines checkpoint therapy-responsive tumor microenvironments. *Nature Medicine*, **24**(8), 1178–1191.

Boissonnas, A., Fetler, L., Zeelenberg, I. S., Hugues, S., & Amigorena, S. (2007). In vivo imaging of cytotoxic T cell infiltration and elimination of a solid tumor. *The Journal of Experimental Medicine*, **204**(2), 345–356.

Brahmer, J. R., Tykodi, S. S., Chow, L. Q., Hwu, W. J., Topalian, S. L., Hwu, P., Drake, C. G., Camacho, L. H., Kauh, J., Odunsi, K., Pitot, H. C., Hamid, O., Bhatia, S., Martins, R., Eaton, K., Chen, S., Salay, T. M., Alaparthy, S., Grosso, J. F., … Wigginton, J. M. (2012). Safety and activity of anti-PD-L1 antibody in patients with advanced cancer. *The New England Journal of Medicine*, **366**(26), 2455–2465.

Breart, B., Lemaitre, F., Celli, S., & Bousso, P. (2008). Two-photon imaging of intratumoral CD8+ T cell cytotoxic activity during adoptive T cell therapy in mice. *The Journal of Clinical Investigation*, **118**(4), 1390–1397.

Cappello, S., Sung, H. M., Ickes, C., Gibhardt, C. S., Vultur, A., Bhat, H., Hu, Z., Brafford, P., Denger, A., Stejerean-Todoran, I., Kohn, R. M., Lorenz, V., Kunzel, N., Salinas, G., Stanisz, H., Legler, T., Rehling, P., Schon, M. P., Lang, K. S., … Bogeski, I. (2021). Protein signatures of NK cell-mediated melanoma killing predict response to immunotherapies. *Cancer Research*, **81**(21), 5540–5554.

Cursons, J., Souza-Fonseca-Guimaraes, F., Foroutan, M., Anderson, A., Hollande, F., Hediyeh-Zadeh, S., Behren, A., Huntington, N. D., & Davis, M. J. (2019). A gene signature predicting natural killer cell infiltration and improved survival in melanoma patients. *Cancer Immunology Research*, **7**(7), 1162–1174.

Derre, L., Corvaisier, M., Charreau, B., Moreau, A., Godefroy, E., Moreau-Aubry, A., Jotereau, F., & Gervois, N. (2006). Expression and release of HLA-E by melanoma cells and melanocytes: potential impact on the response of cytotoxic effector cells. *Journal of Immunology*, **177**(5), 3100–3107.

Dongre, A., & Weinberg, R. A. (2019). New insights into the mechanisms of epithelial-mesenchymal transition and implications for cancer. *Nature Reviews Molecular Cell Biology*, **20**(2), 69–84.

Du, J., Miller, A. J., Widlund, H. R., Horstmann, M. A., Ramaswamy, S., & Fisher, D. E. (2003). MLANA/MART1 and SILV/PMEL17/GP100 are transcriptionally regulated by MITF in melanocytes and melanoma. *The American Journal of Pathology*, **163**(1), 333–343.

Engelhardt, J. J., Boldajipour, B., Beemiller, P., Pandurangi, P., Sorensen, C., Werb, Z., Egeblad, M., & Krummel, M. F. (2012). Marginating dendritic cells of the tumor microenvironment cross-present tumor antigens and stably engage tumor-specific T cells. *Cancer Cell*, **21**(3), 402–417.

Fridman, W. H., Mlecnik, B., Bindea, G., Pages, F., & Galon, J. (2011). Immunosurveillance in human non-viral cancers. *Current Opinion in Immunology*, **23**(2), 272–278.

Fridman, W. H., Zitvogel, L., Sautes-Fridman, C., & Kroemer, G. (2017). The immune contexture in cancer prognosis and treatment. *Nature Reviews Clinical Oncology*, **14**(12), 717–734.

Frisch, J., Angenendt, A., Hoth, M., Prates Roma, L., & Lis, A. (2019). STIM-orai channels and reactive oxygen species in the tumor microenvironment. *Cancers*, **11**(4), 457.

Galon, J., Costes, A., Sanchez-Cabo, F., Kirilovsky, A., Mlecnik, B., Lagorce-Pages, C., Tosolini, M., Camus, M., Berger, A., Wind, P., Zinzindohoue, F., Bruneval, P., Cugnenc, P. H., Trajanoski, Z., Fridman, W. H., & Pages, F. (2006). Type, density, and location of immune cells within human colorectal tumors predict clinical outcome. *Science*, **313**(5795), 1960–1964.

Garner, H., & de Visser, K. E. (2020). Immune crosstalk in cancer progression and metastatic spread: A complex conversation. *Nature Reviews Immunology*, **20**(8), 483–497.

Gocher, A. M., Workman, C. J., & Vignali, D. A. A. (2022). Interferon-gamma: Teammate or opponent in the tumour microenvironment? *Nature Reviews Immunology*, **22**(3), 158–172.

Halle, S., Keyser, K. A., Stahl, F. R., Busche, A., Marquardt, A., Zheng, X., Galla, M., Heissmeyer, V., Heller, K., Boelter, J., Wagner, K., Bischoff, Y., Martens, R., Braun, A., Werth, K., Uvarovskii, A., Kempf, H., Meyer-Hermann, M., Arens, R., … Förster, R. (2016). Vivo killing capacity of cytotoxic t cells is limited and involves dynamic interactions and t cell cooperativity. *Immunity*, **44**(2), 233–245.

Hanahan, D., & Weinberg, R. A. (2011). Hallmarks of cancer: the next generation. *Cell*, **144**(5), 646–674.

Hart, M., Walch-Ruckheim, B., Friedmann, K. S., Rheinheimer, S., Tanzer, T., Glombitza, B., Sester, M., Lenhof, H. P., Hoth, M., Schwarz, E. C., Keller, A., & Meese, E. (2019). miR-34a: A new player in the regulation of T cell function by modulation of NF-kappaB signaling. *Cell Death & Disease*, **10**, 46.

Hernandez, R., Poder, J., LaPorte, K. M., & Malek, T. R. (2022). Engineering IL-2 for immunotherapy of autoimmunity and cancer. *Nature Reviews Immunology*, **22**(10), 614–628.

Hodi, F. S., O'Day, S. J., McDermott, D. F., Weber, R. W., Sosman, J. A., Haanen, J. B., Gonzalez, R., Robert, C., Schadendorf, D., Hassel, J. C., Akerley, W., van den Eertwegh, A. J., Lutzky, J., Lorigan, P., Vaubel, J. M., Linette, G. P., Hogg, D., Ottensmeier, C. H., Lebbe, C., … Urba, W. J. (2010). Improved survival with ipilimumab in patients with metastatic melanoma. *The New England Journal of Medicine*, **363**(8), 711–723.

Holzel, M., & Tuting, T. (2016). Inflammation-induced plasticity in melanoma therapy and metastasis. *Trends in Immunology*, **37**(6), 364–374.

Huang, J., Brameshuber, M., Zeng, X., Xie, J., Li, Q. J., Chien, Y. H., Valitutti, S., & Davis, M. M. (2013). A single peptide-major histocompatibility complex ligand triggers digital cytokine secretion in CD4(+) T cells. *Immunity*, **39**(5), 846–857.

Huergo-Zapico, L., Parodi, M., Cantoni, C., Lavarello, C., Fernandez-Martinez, J. L., Petretto, A., DeAndres-Galiana, E. J., Balsamo, M., Lopez-Soto, A., Pietra, G., Bugatti, M., Munari, E., Marconi, M., Mingari, M. C., Vermi, W., Moretta, L., Gonzalez, S., & Vitale, M. (2018). NK-cell editing mediates epithelial-to-mesenchymal transition via phenotypic and proteomic changes in melanoma cell lines. *Cancer Research*, **78**(14), 3913–3925.

Imai, K., Matsuyama, S., Miyake, S., Suga, K., & Nakachi, K. (2000). Natural cytotoxic activity of peripheral-blood lymphocytes and cancer incidence: An 11-year follow-up study of a general population. *Lancet*, **356**(9244), 1795–1799.

Jenkins, R. W., & Fisher, D. E. (2020). Treatment of advanced melanoma in 2020 and beyond. *The Journal of Investigative Dermatology*, **141**(1), 23–31.

Jobin, G., Rodriguez-Suarez, R., & Betito, K. (2017). Association between natural killer cell activity and colorectal cancer in high-risk subjects undergoing colonoscopy. *Gastroenterology*, **153**(4), 980–987.

Jones, S. A., & Jenkins, B. J. (2018). Recent insights into targeting the IL-6 cytokine family in inflammatory diseases and cancer. *Nature Reviews Immunology*, **18**(12), 773–789.

Kastelan, M., Kovacic, K., Tarle, R., Kraljic, I., & Tarle, M. (1997). Analysis of NK cell activity, lymphocyte reactivity to mitogens and serotest PSA and TPS values in patients with primary and disseminated prostate cancer, PIN and BPH. *Anticancer Research*, **17**, 1671–1675.

Kawakami, Y., Eliyahu, S., Sakaguchi, K., Robbins, P. F., Rivoltini, L., Yannelli, J. R., Appella, E., & Rosenberg, S. A. (1994). Identification of the immunodominant peptides of the MART-1 human melanoma antigen recognized by the majority of HLA-A2-restricted tumor infiltrating lymphocytes. *The Journal of Experimental Medicine*, **180**(1), 347–352.

Khazen, R., Muller, S., Gaudenzio, N., Espinosa, E., Puissegur, M. P., & Valitutti, S. (2016). Melanoma cell lysosome secretory burst neutralizes the CTL-mediated cytotoxicity at the lytic synapse. *Nature Communications*, **7**(1), 10823.

Khazen, R., Muller, S., Lafouresse, F., Valitutti, S., & Cussat-Blanc, S. (2019). Sequential adjustment of cytotoxic T lymphocyte densities improves efficacy in controlling tumor growth. *Scientific Reports*, **9**(1), 12308.

Knorck, A., Marx, S., Friedmann, K. S., Zophel, S., Lieblang, L., Hassig, C., Muller, I., Pilch, J., Sester, U., Hoth, M., Eichler, H., Sester, M., & Schwarz, E. C. (2018). Quantity, quality, and functionality of peripheral blood cells derived from residual blood of different apheresis kits. *Transfusion*, **58**(6), 1516–1526.

Knorck, A., Schafer, G., Alansary, D., Richter, J., Thurner, L., Hoth, M., & Schwarz, E. C. (2022). Cytotoxic efficiency of human CD8(+) t cell memory subtypes. *Frontiers in Immunology*, **13**, 838484.

Kohlhapp, F. J., Broucek, J. R., Hughes, T., Huelsmann, E. J., Lusciks, J., Zayas, J. P., Dolubizno, H., Fleetwood, V. A., Grin, A., Hill, G. E., Poshepny, J. L., Nabatiyan, A., Ruby, C. E., Snook, J. D., Rudra, J. S., Schenkel, J. M., Masopust, D., Zloza, A., & Kaufman, H. L. (2015). NK cells and CD8+ T cells cooperate to improve therapeutic responses in melanoma treated with interleukin-2 (IL-2) and CTLA-4 blockade. *Journal for Immunotherapy of Cancer*, **3**(1), 18.

Krysan, K., Tran, L. M., Grimes, B. S., Fishbein, G. A., Seki, A., Gardner, B. K., Walser, T. C., Salehi-Rad, R., Yanagawa, J., Lee, J. M., Sharma, S., Aberle, D. R., Spira, A. E., Elashoff, D. A., Wallace, W. D., Fishbein, M. C., & Dubinett, S. M. (2019). The immune contexture associates with the genomic landscape in lung adenomatous premalignancy. *Cancer Research*, **79**(19), 5022–5033.

Kucera, R., Topolcan, O., Treskova, I., Kinkorova, J., Windrichova, J., Fuchsova, R., Svobodova, S., Treska, V., Babuska, V., Novak, J., & Smejkal, J. (2015). Evaluation of IL-2, IL-6, IL-8 and IL-10 in malignant melanoma diagnostics. *Anticancer Research*, **35**, 3537–3541.

Kummerow, C., Schwarz, E. C., Bufe, B., Zufall, F., Hoth, M., & Qu, B. (2014). A simple, economic, time-resolved killing assay. *European Journal of Immunology*, **44**(6), 1870–1872.

Le, D. T., Burt, B., Van Buren, G., Abeynaike, S., Zalfa, C., Nikzad, R., Kheradmand, F., & Paust, S. (2020). NK cells and CTLs are required to clear solid tumor in a novel model of patient-derived-xenograft. *bioRxiv*, https://doi.org/10.1101/2020.05.24.112722

Lee, J. H., Park, S., Cheon, S., Lee, J. H., Kim, S., Hur, D. Y., Kim, T. S., Yoon, S. R., Yang, Y., Bang, S. I., Park, H., Lee, H. T., & Cho, D. (2011). 1,25-Dihydroxyvitamin D(3) enhances NK susceptibility of human melanoma cells via Hsp60-mediated FAS expression. *European Journal of Immunology*, **41**(10), 2937–2946.

Li, F. Z., Dhillon, A. S., Anderson, R. L., McArthur, G., & Ferrao, P. T. (2015). Phenotype switching in melanoma: Implications for progression and therapy. *Frontiers in Oncology*, **5**, 31.

Lorenzo-Herrero, S., Lopez-Soto, A., Sordo-Bahamonde, C., Gonzalez-Rodriguez, A. P., Vitale, M., & Gonzalez, S. (2018). NK cell-based immunotherapy in cancer metastasis. *Cancers*, **11**(1), 29.

Malmberg, K. J., Levitsky, V., Norell, H., de Matos, C. T., Carlsten, M., Schedvins, K., Rabbani, H., Moretta, A., Soderstrom, K., Levitskaya, J., & Kiessling, R. (2002). IFN-gamma protects short-term ovarian carcinoma cell lines from CTL lysis via a CD94/NKG2A-dependent mechanism. *The Journal of Clinical Investigation*, **110**(10), 1515–1523.

Mempel, T. R., Pittet, M. J., Khazaie, K., Weninger, W., Weissleder, R., von Boehmer, H., & von Andrian, U. H. (2006). Regulatory T cells reversibly suppress cytotoxic T cell function independent of effector differentiation. *Immunity*, **25**(1), 129–141.

Miettinen, P. J., Ebner, R., Lopez, A. R., & Derynck, R. (1994). TGF-beta induced transdifferentiation of mammary epithelial cells to mesenchymal cells: Involvement of type I receptors. *The Journal of Cell Biology*, **127**(6), 2021–2036.

Mittal, V. (2018). Epithelial MESENCHYMAL TRANSITION IN TUMOR METAStasis. *Annual Review of Pathology*, **13**(1), 395–412.

Muenst, S., Laubli, H., Soysal, S. D., Zippelius, A., Tzankov, A., & Hoeller, S. (2016). The immune system and cancer evasion strategies: Therapeutic concepts. *Journal of Internal Medicine*, **279**(6), 541–562.

Neubert, N. J., Soneson, C., Barras, D., Baumgaertner, P., Rimoldi, D., Delorenzi, M., Fuertes Marraco, S. A., & Speiser, D. E. (2016). A well-controlled experimental system to study interactions of cytotoxic t lymphocytes with tumor cells. *Frontiers in Immunology*, **7**, 326.

O'Donnell, J. S., Teng, M. W. L., & Smyth, M. J. (2019). Cancer immunoediting and resistance to T cell-based immunotherapy. *Nature Reviews Clinical Oncology*, **16**(3), 151–167.

Ochayon, D. E., & Waggoner, S. N. (2021). The effect of unconventional cytokine combinations on NK-cell responses to viral infection. *Frontiers in Immunology*, **12**, 645850.

Orr, M. T., & Lanier, L. L. (2010). Natural killer cell education and tolerance. *Cell*, **142**(6), 847–856.

Pietra, G., Manzini, C., Rivara, S., Vitale, M., Cantoni, C., Petretto, A., Balsamo, M., Conte, R., Benelli, R., Minghelli, S., Solari, N., Gualco, M., Queirolo, P., Moretta, L., & Mingari, M. C. (2012). Melanoma cells inhibit natural killer cell function by modulating the expression of activating receptors and cytolytic activity. *Cancer Research*, **72**(6), 1407–1415.

Prager, I., & Watzl, C. (2019). Mechanisms of natural killer cell-mediated cellular cytotoxicity. *Journal of Leukocyte Biology*, **105**(6), 1319–1329.

Purbhoo, M. A., Irvine, D. J., Huppa, J. B., & Davis, M. M. (2004). T cell killing does not require the formation of a stable mature immunological synapse. *Nature Immunology*, **5**(5), 524–530.

Ribas, A., & Wolchok, J. D. (2018). Cancer immunotherapy using checkpoint blockade. *Science*, **359**(6382), 1350–1355.

Romero, P., Gervois, N., Schneider, J., Escobar, P., Valmori, D., Pannetier, C., Steinle, A., Wolfel, T., Lienard, D., Brichard, V., van Pel, A., Jotereau, F., & Cerottini, J. C. (1997). Cytolytic T lymphocyte recognition of the immunodominant HLA-A*0201-restricted Melan-A/MART-1 antigenic peptide in melanoma. *Journal of Immunology*, **159**, 2366–2374.

Rosenberg, J., & Huang, J. (2018). CD8(+) T cells and NK cells: Parallel and complementary soldiers of immunotherapy. *Current Opinion in Chemical Engineering*, **19**, 9–20.

Salter, R. D., & Cresswell, P. (1986). Impaired assembly and transport of HLA-A and -B antigens in a mutant TxB cell hybrid. *The EMBO Journal*, **5**(5), 943–949.

Schadendorf, D., van Akkooi, A. C. J., Berking, C., Griewank, K. G., Gutzmer, R., Hauschild, A., Stang, A., Roesch, A., & Ugurel, S. (2018). Melanoma. *Lancet*, **392**(10151), 971–984.

Shankaran, V., Ikeda, H., Bruce, A. T., White, J. M., Swanson, P. E., Old, L. J., & Schreiber, R. D. (2001). IFNgamma and lymphocytes prevent primary tumour development and shape tumour immunogenicity. *Nature*, **410**(6832), 1107–1111.

Sugita, S., Sagawa, K., Mochizuki, M., Shichijo, S., & Itoh, K. (1996). Melanocyte lysis by cytotoxic T lymphocytes recognizing the MART-1 melanoma antigen in HLA-A2 patients with Vogt-Koyanagi-Harada disease. *International Immunology*, **8**(5), 799–803.

Tarazona, R., Duran, E., & Solana, R. (2015). Natural killer cell recognition of melanoma: New clues for a more effective immunotherapy. *Frontiers in Immunology*, **6**, 649.

Tekpli, X., Lien, T., Rossevold, A. H., Nebdal, D., Borgen, E., Ohnstad, H. O., Kyte, J. A., Vallon-Christersson, J., Fongaard, M., Due, E. U., Svartdal, L. G., Sveli, M. A. T., Garred, O., Osbreac, F. A., Sahlberg, K. K., Sorlie, T., Russnes, H. G., Naume, B., & Kristensen, V. N. (2019). An independent poor-prognosis subtype of breast cancer defined by a distinct tumor immune microenvironment. *Nature Communications*, **10**(1), 5499.

Trucco, L. D., Mundra, P. A., Hogan, K., Garcia-Martinez, P., Viros, A., Mandal, A. K., Macagno, N., Gaudy-Marqueste, C., Allan, D., Baenke, F., Cook, M., McManus, C., Sanchez-Laorden, B., Dhomen, N., & Marais, R. (2019). Ultraviolet radiation-induced DNA damage is prognostic for outcome in melanoma. *Nature Medicine*, **25**(2), 221–224.

Viros, A., Sanchez-Laorden, B., Pedersen, M., Furney, S. J., Rae, J., Hogan, K., Ejiama, S., Girotti, M. R., Cook, M., Dhomen, N., & Marais, R. (2014). Ultraviolet radiation accelerates BRAF-driven melanomagenesis by targeting TP53. *Nature*, **511**(7510), 478–482.

Walwyn-Brown, K., Pugh, J., Cocker, A. T. H., Beyzaie, N., Singer, B. B., Olive, D., Guethlein, L. A., Parham, P., & Djaoud, Z. (2022). Phosphoantigen-stimulated gammadelta t cells suppress natural killer-cell responses to missing-self. *Cancer Immunology Research*, **10**(5), 558–570.

Weigelin, B., den Boer, A. T., Wagena, E., Broen, K., Dolstra, H., de Boer, R. J., Figdor, C. G., Textor, J., & Friedl, P.. (2021). Cytotoxic T cells are able to efficiently eliminate cancer cells by additive cytotoxicity. *Nature Communications*, **12**, 5217. https://doi.org/10.1038/s41467-021-25282-3

Wolfl, M., & Greenberg, P. D. (2014). Antigen-specific activation and cytokine-facilitated expansion of naive, human CD8+ T cells. *Nature Protocols*, **9**(4), 950–966.

Xu, D., Gu, P., Pan, P. Y., Li, Q., Sato, A. I., & Chen, S. H. (2004). NK and CD8+ T cell-mediated eradication of poorly immunogenic B16-F10 melanoma by the combined action of IL-12 gene therapy and 4-1BB costimulation. *International Journal of Cancer*, **109**(4), 499–506.

Zippelius, A., Pittet, M. J., Batard, P., Rufer, N., de Smedt, M., Guillaume, P., Ellefsen, K., Valmori, D., Lienard, D., Plum, J., MacDonald, H. R., Speiser, D. E., Cerottini, J. C., & Romero, P. (2002). Thymic selection generates a large T cell pool recognizing a self-peptide in humans. *The Journal of Experimental Medicine*, **195**(4), 485–494.

Additional information

Data availability statement

All data with $n < 30$ are made available according to the guidelines. The mean, SD and n are always provided.

Competing interests

None.

Author contributions

K.S.F., C.K., E.C.S. and M.H. were responsible for conception or design of the work, with help from all authors regarding certain aspects. K.S.F. performed and analysed most experiments. L.K., N.K. and N.L. contributed to the experiments shown in Figs 6 and 7 and performed all cytokine assays. A.K. contributed

to and analysed experiments shown in Fig. 2 and flow cytometry data. S.C. designed the assay for SK-Mel-5–NK cell co-culture under supervision by C.K. and I.B. C.H. and G.S. helped with generation of MART-1-specific CTL clones. All authors analysed and/or interpreted certain parts of the work. S.I. helped with interpretation of data, conception of the paper and editing of the manuscript. K.S.F., L.K. and A.K. co-wrote the Methods section, with corrections from E.C.S. and M.H. M.H. drafted the paper, with help from K.S.F., E.C.S., A.K., S.I. and all other authors. All authors edited and discussed the manuscript and the analysis of the data. All authors approved the final version of the manuscript and agree to be accountable for all aspects of the work in ensuring that questions related to the accuracy or integrity of any part of the work are appropriately investigated and resolved. All persons designated as authors qualify for authorship, and all those who qualify for authorship are listed.

Funding

This project was funded by grants from the Deutsche Forschungsgemeinschaft (DFG): SFB 1027 (project A2 to Bin Qu and M.H., project A11 to M.H., project A12 to S.I., and project C4 to I.B.) and SFB 894 (project A1 to M.H.) and Major Instrumentation grants INST256/429-1 FUGB (Molecular Devices, High content Screening System) and INST 256/423-1 FUGG (BD Biosciences, FACSVerse). It was also funded by the Bundesministerium für Bildung und Forschung (BMBF, grant 031LO133 to M.H.).

Acknowledgements

We appreciate the help of Professor Hermann Eichler and the Institute of Clinical Hemostaseology and Transfusion Medicine at Saarland University Medical Centre for obtaining human blood cells. We thank PD Dr Frank Neumann (José Carreras Centre, Saarland University Medical Centre, Homburg, Germany) for providing T2 target cells and Epstein–Barr virus-transformed B lymphoblastoid cell lines. We gratefully acknowledge Carmen Hässig for cell preparation. We also thank Elmar Krause and Jens Rettig for allowing us to use the flow cytometric sorting facility. We thank all laboratory members for insightful discussions.

Open Access funding enabled and organized by Projekt DEAL.

Keywords

cancer cells, cytotoxic efficiency, cytotoxic T lymphocytes, human leucocyte antigen, immune evasion, interleukin-6, MART-1, melanoma, natural killer cells, resistance

Supporting information

Additional supporting information can be found online in the Supporting Information section at the end of the HTML view of the article. Supporting information files available:

Statistical Summary Document
Peer Review History

Translational perspective

Immune cell therapies have emerged as powerful tools against different cancers. Among those are therapies with T lymphocytes including chimeric antigen receptor (CAR) T cells. Recently, also therapies with natural killer (NK) cells have gained more attention. It is a matter of time until cytotoxic T lymphocytes (CTL) and NK cells will be combined in therapies. This is an attractive scenario as not all patients respond to single therapies equally well, and combinatorial therapies have long been used successfully in cancer therapy. To optimize CTL and NK cell numbers for therapy and the timing of application, in vitro assays with human cells might prove very useful. In the present report, we present an assay that is well-suited to test the combined therapy with NK cells and CTL. Importantly our data also makes predictions about the optimal order of NK cell and CTL treatment, and it could be explored to suggest optimal time points and cell numbers. We are optimistic that the assay and the results on interdependencies will help to understand and optimize future immune therapies against cancer.